Article

A Multi-disciplinary Modelling Approach for Discharge Reconstruction in Irrigation Canals: The Canale Emiliano Romagnolo (Northern Italy) Case Study

Marta Luppi [1], Pierre-Olivier Malaterre [2], Adriano Battilani [3], Vittorio Di Federico [4] and Attilio Toscano [1,*]

[1] Department of Agricultural and Food Sciences, University of Bologna, Viale Giuseppe Fanin 50, 40127 Bologna, Italy; marta.luppi2@unibo.it
[2] UMR G-eau, IRSTEA, 361 rue Jean-François Breton, 34196 Montpellier, France; pierre-olivier.malaterre@irstea.fr
[3] Consorzio del Canale Emiliano Romagnolo (CER), via Ernesto Masi 8, 40137 Bologna, Italy; battilani@consorziocer.it
[4] Department of Civil, Chemical, Environmental and Materials Engineering, University of Bologna, Viale Risorgimento 2, 40136 Bologna, Italy; vittorio.difederico@unibo.it
* Correspondence: attilio.toscano@unibo.it; Tel.: +39-051-2096179

check for updates

Abstract: Agriculture is the biggest consumer of water in the world, and therefore, in order to mitigate the effects of climate change, and consequently water scarcity, it is important to reduce irrigation water losses and to improve the poor collection of hydraulic status data. Therefore, efficiency has to be increased, and the regulation and control flow should be implemented. Hydraulic modelling represents a strategic tool for the reconstruction of the missing hydraulic data. This paper proposes a methodology for the unmeasured offtake and flowing discharge estimation along the open-canal Canale Emiliano Romagnolo (CER), which is one of the major irrigation infrastructures in Northern Italy. The "multi-disciplinary approach" that was adopted refers to agronomic and hydraulic aspects. The tools that were used are the IRRINET management Decisional Support System (DSS) and the SIC^2 (Simulation and Integration of Control for Canals) hydraulic software. Firstly, the methodology was developed and tested on a Pilot Segment (PS), characterized by a simple geometry and a quite significant historical hydraulic data availability. Then, it was applied on an Extended Segment (ES) of a more complex geometry and hydraulic functioning. Moreover, the available hydraulic data are scarce. The combination of these aspects represents a crucial issue in the irrigation networks in general.

1. Introduction

Counting on the intensive exploitation of the water resources, many works of the last decades have addressed agricultural water management practices towards the productivity strengthening and the defeating poverty [1–3]. Nowadays, the water scarcity, combined with the rising food demand, has involved a gradual switch of the objectives [1,3] to the following: Resource preservation (quantitatively, qualitatively, and ecologically) in relation to agricultural production (crop irrigation, animal rearing, and on-farm operations) [4–6], rural realities economy improvement [7,8], and facing climate change [9].

The sustainable development resulted from these key components is promoted by the Water Framework Directive (WFD/2000/60CE) [10] and policies that are closely related to the EU2020 program [11–13]. At the regional scale, the water management practices for irrigation are identified as a primary challenge because of their socio-economic implications [13]. They consist in the improvement of the irrigation consumption knowledge at the field scale and the increase in the efficiency and the discharge regulation at conveyance system scale [14].

Despite the evolution of irrigation infrastructures tends to be focused mainly on pressurized systems, many districts are often fed by dense canal networks that have remained basically unchanged since they were constructed decades ago. They are characterized by significant water losses and irrecoverable outflow at their end [15–18]. The irrigation systems performances can be improved through hardware (physical/structural) changes, such as the canal lining or the installation of sophisticated control structures [19,20], or through software (operational) techniques, such as appropriate delivery rules and an effective communication between water supply agencies and water users [21].

A common flaw in irrigation delivery systems that are characterized by open canals and by many users is the absence of a proper information system that ensures and collects measured and monitored data about hydraulic status [22–25]. When considering that the total water consumption for irrigation is projected to increase by 10% by 2050 [26], it will represent a central issue in the near future [27]. Generally, the only known quantities are measured water levels at specific locations, often with limited precision and possible failures [19].

Hydraulic modelling emerges as a strategic tool for: 1) the reconstruction of unmeasured data, such as discharges or water levels at other locations, unknown perturbations (inflows and outflows) [28,29], and hydraulic variables (friction coefficients and hydraulic device discharge coefficients) [19,30]. 2) the visualization and control of the flow at several structures [15,31].

In parallel, irrigation Decisional Support Systems (DSS) can characterize the crops that are served by a specific irrigation delivery system, and also, can indirectly monitor their hydraulic status. In the last few decades, DSS underwent many changes [32,33] ranging from the prevention of extreme events (droughts and floods) and pollution [32] to the irrigation scheduling [34–39]. The latter is based on the integration of several models, processes, and factors (i.e., meteorological and soil conditions and types of crops) [40,41].

This study presents a tool for the reconstruction of unmeasured discharges along a specific irrigation delivery canal. The combination of hydraulic modelling and irrigation DSS can solve the problem that was created by the poor hydraulic data collection. The multi-disciplinary approach that is proposed in this paper reflects the merging of hydraulic engineering and agronomy aspects. It was developed on one of the most important irrigation canals in Northern Italy: The Canale Emiliano Romagnolo (CER) [42]. The methodology was developed on a simple geometry 7 km long Pilot Segment (PS) and over a more complex 22 km long Extended Segment (ES).

2. Materials and Methods

2.1. Description of the CER

The CER starts in Salvatonica di Bondeno (Ferrara, Italy) on the right bank of the Po River and it provides the irrigation supply for an area of about 3000 km^2. That area represents the 93% of the irrigated and the 22% of the agricultural land in the Emilia Romagna Region. The agricultural land covers the 60% of the regional territory [43], where different cultures are irrigated, among which extensive crops, vegetables, and orchards [44]. To convey and to distribute water, the CER hydraulic system uses seven pumping stations (the main one on the Po River) and 165 km of canal networks (Figure 1).
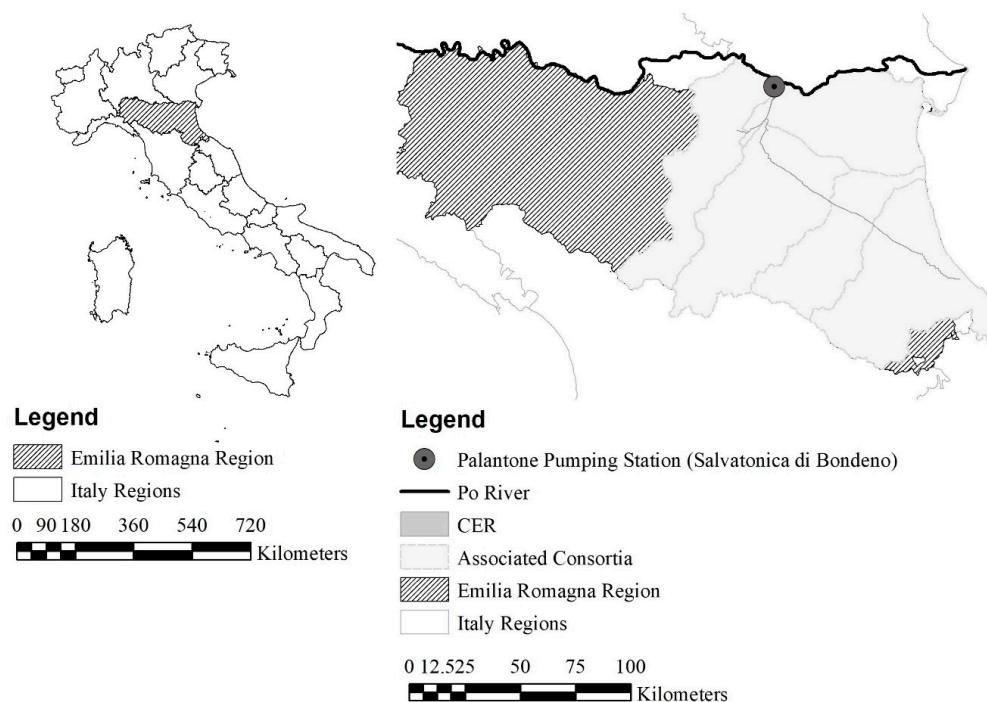
Figure 1. The Emilia Romagna Region, the Associated Consortia and the CER.

The main reach is 133 km long and its first 104 km are characterized by 60–17.6 m width at the top and 6.0–6.4 m at the bottom of the canal. The side slopes are 3:1 and 1.5:1 or 1.75:1 for composite trapezium sections (first 37 km) and 2:1 for the simple ones. The cross section of the canal later becomes narrower with a rectangular shape: open (width range: 6.8–5.6 m, elevation range: 3–2.7 m) or closed (width range: 6.4–5.6 m, elevation range: 2.1–1.9 m) and made of reinforced concrete. The CER receives no inflow from surface runoff, drainage, or different types of discharges, but it has several offtakes. From the canal, the water is offtake using pumps or gates, and it is conveyed to the irrigated fields through secondary channels that are managed by Associated Consortia. The irrigation offtakes have a seasonal variability, and therefore the maximum permitted discharge at the main pumping station varies from 68 m^3/s (from May to September) to 25 m^3/s (the rest of the year). Moreover, discharges are also affected by the meteorological issues (e.g., long dry seasons), the type of cultivated crops, and the irrigation practices. The Consortium of the CER is in charge of: (1) maintenance operations (geometric and functioning repairs, periodic cleanings); (2) collection of quantitative and qualitative measurements; and, (3) supply of irrigation services to farmers (by means of several irrigation Associated Consortia that distributes water to final users).

2.2. Investigation Period and Available Data

This study focuses on the period of full operation of the CER i.e., the irrigation season (June–August) that is characterized by the highest water demand and irrigation frequency. The irrigation period selected comprises 73 days (20 June–31 August) of the years from 2012 to 2015. These years were characterized by different average daily rainfall. For example, 2013 (1.30 mm/day) and 2015 (0.94 mm/day) had daily rainfall that was close to the decennial (2005–2015) average value (1.1 mm/day), while 2014 (2.22 mm/day) and 2012 (0.13 mm/day) were especially rainy and dry, respectively.

The main available data for this study are: (1) water volumes at offtakes (calculated indirectly); (2) crop water requirements (estimated); and, (3) water levels at the main canal (measured); (4) functioning data of pumping stations along the CER (measured).

In particular, for each irrigation offtake, calculated and estimated water amounts were provided. The former refers to monthly cumulated volumes indirectly calculated by the Associated Consortia on the basis of flow rates and working times of offtakes pumps or the opening gate area, the opening time, and the water level at offtakes manual gates.

On the other hand, estimated water volumes were based on the crop water requirements provided by the IRRINET management DSS, which was developed by the Consortium of the CER [45]. IRRINET is identified as the reference tool for the estimation of irrigation volumes in the Emilia Romagna Region [46], and it provides to farmers a day-by-day information on how much and when to irrigate crops [47]. It is based on a daily water balance of soil-plant-atmosphere system. IRRINET processes a huge quantity of information related to: areas (meteorological, water table depth and soil data) and farms (types of irrigated crops, start and stop crops dates). Since 2012, at the end of every irrigation period, the Consortium of the CER has collected daily optimum crop water requirement (*CWR*) values for all the crops that are served by IRRINET. For every type of crop (*i*) and for every day, these values are averaged; afterwards, they are cumulated on a decadal time scale giving CWR_i (Section 2.4.1).

Along the CER, the only hydraulic measurements available are water levels. In total, forty cross-sections are equipped with ultrasonic level transmitters (The Probe PL-517, Terry Ferraris &C. S.p.A., Milan, Italy). These instruments are generally located near two types of infrastructures: (a) culverts (passing under different rivers; in total, 29 instruments); and (b) pumping stations (in suctions and/or delivery tanks; in total 11 instruments). After direct field surveys, the measurement accuracy of both types of transmitters was estimated to be lower than the original instrument accuracy (±0.02 m), in particular, ±0.05 m and ±0.10 m, respectively. The transmitters located near culverts serve for management purposes, and their accuracy was probably affected by flow disturbances (sediment build up and depressions next to the edges of culverts entrances due to velocity changes) [48]. On the other hand, the transmitters near pumping stations are used for operational purposes and they are strongly influenced by the pumps functioning.

At each of the 40 cross-sections, the water level value is transmitted and is registered with a time step of 30 min. Because of the offtake data time scale (monthly or decadal) and because of the general water level series incompleteness, the 30 min available measures were averaged on a daily time scale.

Finally, the daily measured functioning data at one pumping station (Pieve di Cento) were investigated (Section 2.6). Every time that the installed pumps would turn on or turn off the following parameters were measured: voltage (V), electric current (A), functioning time (h), discharge (m^3/s), volume (m^3), suction, and delivery tanks water level (m).

Table 1 provides a summary of all the available data used in the present application.

Table 1. The available data and their characteristics.

Available Data	Type	Unit	Time Step	Source
Offtake Volumes	Indirectly calculated	m^3	Monthly (cumulated values)	Associated Consortia
CWR_i	Estimated	mm	Decadal (cumulated values)	IRRINET
Water Levels	Measured	m	Daily (average values)	CER
Water Levels at Suction/Delivery Tanks	Measured	m	Pumps on/off (single values)	CER

2.3. Description of the Pilot Segment (PS)

The multi-disciplinary modelling approach was developed on a 7 km long Pilot Segment (PS) of the CER.

The PS extremities coincide with two concrete culverts called Culv_1 (upstream) and Culv_2 (downstream) (Figure 2). They are characterized by rectangular flow sections of 36 m^2 and of 31.5 m^2,

respectively, and by submerged entrances and surface or/and piped-flow conditions. PS has three different trapezium cross sections with width ranges of 22.8–25.8 m (at the top) and 3.3–7 m (at the bottom). The side slopes are 3:1 and 1.5:1 for the first composite cross section and 2:1 for the other two simple sections. For the first 700 m along the segment, the bed altimetry goes from 12.81 m to 13.74 m above the sea level. After that part, the canal has a constant slope with a final value of 13.32 m above sea level.
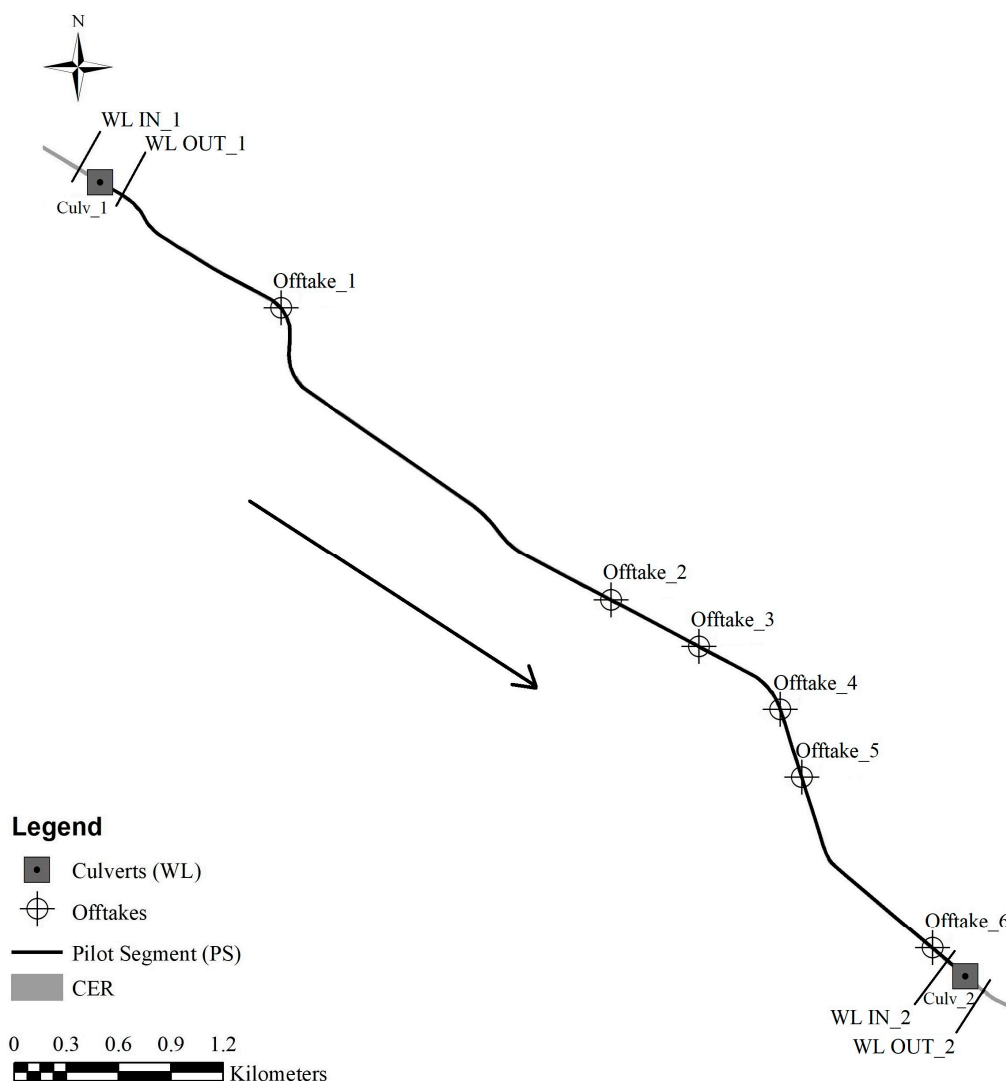

Figure 2. The scheme of Pilot Segment (PS): The six irrigation offtakes, the two culverts passing under the Idice River (Culv_1) and the Quaderna River (Culv_2), the four water gauges (WL) at the IN and OUT of both the culverts.

Six offtakes of PS serve a large irrigated area (8385 ha) through a network of not-pressurized irrigation channels. Over the four years of analysis, the biggest amount of water diverted from the segment (70% of the total offtake), was always diverted by the same three offtakes out of the six mentioned. The water gauges present at the segment are four: two at Culv_1 and two at Culv_2. They are located a few meters away from the entrance and the exit of both culverts (Figure 2).

2.4. Elaboration of the Multi-Disciplinary Modelling Approach on PS

The methodology was developed on a 7 km long Pilot Segment (PS), which was characterized by a simple geometry and a quite significant availability of water level measurements. The offtake

discharges were estimated and verified also while considering the daily optimum *CWR* at field scale [46], that was estimated by the IRRINET, a regional irrigation DSS [45]. Combining hydraulic modelling of the CER with the optimization process of the hydraulic variables (Manning's coefficient and gate discharge coefficient) allowed for determining the flowing discharges. The simulations were run under steady flow conditions using the hydraulic software SIC^2 (5.38c, UMR G-eau IRSTEA, Montpellier, France) [49].

The methodology developed on PS was later applied on a 22 km Extended Segment (ES), that apart from a more complex geometry and hydraulic functioning (especially because of the presence of four culverts), also has a lower hydraulic data availability and lower accuracy when compared to PS. The methodology was tested on this particular segment, since it was characterized by different issues that are common in irrigation networks [19].

2.4.1. Reconstruction of the Unmeasured Offtake Discharges

The offtakes that were not measured were reconstructed using the indirectly calculated and the estimated data provided by the Associated Consortia and by the IRRINET service, respectively. In the following description, in order to distinguish these two data sources, different indexes are used: *D* for the former (Associated Consortia) and *T* for the latter (IRRINET). The index *C* indicates the results that were obtained by calculations done by the authors with the available data. The *T*-data aim to refine the time scale of the *D*-data and to verify them by a comparison with agronomic values, such as crop water requirements. Therefore, the obtained *C*-results (Equations (1)–(3)) have a decadal time scale instead of a monthly one; moreover, their values include agronomic aspects (e.g., optimum crop water requirement), the intensity, and the efficiency of the irrigation practices (Equation (4)).

During the decade *n*, the discharge exiting from a generic offtake *k*, q_{kCn} (m^3/s) can be written as:

$$q_{kCn} = q_{rDm}\, w_{kCn} \tag{1}$$

where q_{rDm} (m^3/s) is the average discharge diverted from the reference offtake during the month *m* (*m* = 1, 2, 3), and w_{kCn} is the weight of the offtake *k* during the decade *n* (*n* = 1, ..., 7).

The reference offtake was identified every year as the one diverting the greatest irrigation water volume. q_{rDm} was calculated as:

$$q_{rDm} = \frac{V_{rDm}}{D_m} \tag{2}$$

where V_{rDm} (m^3) is the indirectly calculated cumulated volume of the reference offtake for the month *m*, while D_m (s) is the duration of the month *m*.

The weight was obtained comparing the offtake *k* and the reference offtake in volumetric terms. The approach considered w_{kCn}, as follow:

$$w_{kCn} = \frac{(w_{kDm} + w_{kTn})}{2}; \; w_{kDm} = \frac{V_{kDm}}{V_{rDm}}; \; w_{kTn} = \frac{V_{kTn}}{V_{rTn}} \tag{3}$$

where w_{kDm} (-) and w_{kTn} (-) are the weights of the offtake *k* obtained using the *D*-data and the *T*-data, respectively, V_{kDm} (m^3) is the indirectly calculated volume of the offtake *k* during the month *m*, V_{kTn} (m^3), and V_{rTn} (m^3) are the volumes of the offtake *k* and of the reference offtake, respectively, calculated during the decade *n* using IRRINET.

In particular, for the decade *n*, the calculated volume of the generic offtake *k* (V_{kTn}) was determined by the expression [14]:

$$V_{kTn} = \left[\sum_{i=1}^{n} \left(\frac{CWR_i\, A_i\, II_i}{EI_i} \right) \right] \frac{1}{ED} \tag{4}$$

where A_i (m^2) is the area covered by the crop i per each year, CWR_i (mm) is the decadal cumulated optimum water requirement for the crop i, II_i (-) is the irrigation intensity of the crop i, EI_i (-) is the efficiency of the irrigation method for the crop i, and ED (-) is the efficiency of the delivery system.

If the generic offtake k is the reference offtake, the Equation (4) gives the quantity V_{rTn}.

The *CWR* values were provided by the Consortium of the CER, as already said in Section 2.2 for extensive cultivations (maize, soy, and alfa-alfa), for vegetables (beet, onion, melon, potato, and tomato), and for orchards (pear-tree, peach-tree, and vine).

The coefficient *II* indicates the intensity of irrigation, in other words, the ratio between the irrigated area and the area that potentially could be irrigated [50–52]. Its values were determined through field studies at the regional scale [53–56]. In particular, for the involved case-study crops, *II* ranges from 0.25 to 1, as shown in Table 2.

The coefficient *EI* indicates the efficiency of the irrigation method [57]. In Emilia Romagna, the considered value ranges are: 0.85–0.90 for drip irrigation and 0.70–0.80 for sprinkling irrigation [58]. In Table 2, the values of 0.85 and 0.75 were adopted for crops that were under the former and the latter irrigation efficiency, respectively.

The coefficient *ED* indicates the efficiency of the system that conveys water from the offtakes on the banks of the CER to the fields. For the present case-study, it was considered to be 0.50 [59,60]. In the area, in fact, 1122 km of channels (for both irrigation and drainage) and only 235 km of pipes provide water for crops. In particular, non-lined channels realize the 88% of the irrigation distribution [61].

Table 2. The values of the coefficients intensity of irrigation *(II)* and efficiency of the irrigation method *(EI)* for the irrigated crops served by PS and extended segment (ES).

Irrigated Crops	II_i (-)	EI_i (-)
Extensive crops		
Maize	0.75	0.75
Soy	0.50	0.75
Alfa-Alfa	0.25	0.75
Vegetables		
Beet	0.60	0.75
Onion	1.00	0.75
Melon	1.00	0.85
Potato	1.00	0.75
Tomato	1.00	0.85
Orchards		
Pear	1.00	0.85
Peach	1.00	0.85
Vine	0.50	0.85

2.4.2. Reconstruction of the Unmeasured Flowing Discharges

The hydraulic modelling combined with hydraulic variables optimization processes allowed for reconstructing the unmeasured flowing discharges along the segment.

SIC^2 (Simulation and Integration of Control for Canals) was selected as the most appropriate irrigation canal modelling software. It has been developed at IRSTEA (previously CEMAGREF, Montpellier, France) [62] and it enables describing the dynamics of rivers, drainage networks, and irrigation canals [63]. For the latter, devices (i.e., sills and gates) and irrigation offtakes can be specified in geometric and functioning terms [49]. SIC^2 can run steady flow computations under boundary conditions for discharge and/or water level [64]. In fact, it can consider several combinations of settings for devices and offtakes. The software provides the water level and the discharge profiles along the analyzed hydraulic system [29]. SIC^2 models also unsteady flow for initial conditions that were obtained from steady state computations [64] in discharge and water level terms. It can be used for water demand and control operations [19,65]. SIC^2 describes the dynamic behavior of water (discharge

and water level) with the complete one-dimensional (1-D) Saint Venant equations in a bounded system [49]. This is the case of the CER in which the flow can be considered as mono-dimensional with a direction sufficiently rectilinear.

The 1-D Saint Venant equations are mathematically expressed as [66]:

$$\frac{\partial Q}{\partial x} + \frac{\partial S}{\partial t} = 0 \tag{5}$$

$$\frac{\partial Q}{\partial t} + \frac{\partial (Q^2/S)}{\partial x} + g\, S\, \frac{\partial Z}{\partial x} + g\, S\, J = 0 \tag{6}$$

where Q (m^3/s) is the discharge, S (m^2) is the wetted area, g (m/s^2) is the acceleration due to gravity, Z (m) is the water level, J (m/m) is the friction slope, x (m) is the longitudinal abscissa, and t (s) is the time.

The friction slope is obtained by the Manning-Strickler formula:

$$J = \frac{n^2\, Q^2}{S^2\, R^{4/3}} \tag{7}$$

where n (m$^{1/3}$/s) is the Manning's coefficient and R (m) is the hydraulic radius.

The continuity (Equation (5)) and the momentum (Equation (6)) equations are completed by boundary conditions for which SIC^2 provides a large range of options. They can be imposed in discharge, elevation, or rating curve terms. Lateral inflows and weir and gate equations can also be inserted. For example, the flow through a gate structure can be expressed by several classical or advanced equations, such as the submerged flow equation:

$$Q = C_d\, \sqrt{2\, g}\, L\, u\, \sqrt{Z_{up} - Z_{dn}} \tag{8}$$

where C_d (-) is the gate discharge coefficient, L (m) is the gate width, u (m) is the gate opening, Z_{up} (m), and Z_{dn} (m) are the water levels at the upstream and at the downstream of the gate, respectively.

The Saint Venant equations are non-linear partial differential equations and an analytical solution is restricted to problems of simple geometry. For all other cases, implicit finite difference approximations and a Preissmann scheme are used, as in the case of SIC^2 [66–68].

After the PS geometry entry, several hydraulic aspects were evaluated in SIC^2. The hydraulic variables values were set according to the literature: The Manning's coefficient presented a constant value of 0.013 (m$^{1/3}$/s) along the segment and within the two culverts [68] and the gate discharge coefficient that characterizes the entrances of each culvert was 0.6 [16,49,69]. The offtakes were modelled as "nodes" and they were characterized in discharge terms. In particular, the q_{kCn} values were inserted and were linearly interpolated in time.

For the year y, the vectors $Z1_{obs,y}$, $Z2_{obs,y}$, $Z3_{obs,y}$, and $Z4_{obs,y}$ can be defined. They contain the daily measured water levels at the four gauges: WL IN_1, WL OUT_1, WL IN_2, and WL OUT_2, respectively (Figure 2).

$$Z1_{obs,y} = \begin{pmatrix} Z1_{obs_1} \\ Z1_{obs_2} \\ Z1_{obs_j} \\ .. \\ Z1_{obs_e} \end{pmatrix} ; Z2_{obs,y} = \begin{pmatrix} Z2_{obs_1} \\ Z2_{obs_2} \\ Z2_{obs_j} \\ .. \\ Z2_{obs_e} \end{pmatrix} ; Z3_{obs,y} = \begin{pmatrix} Z3_{obs_1} \\ Z3_{obs_2} \\ Z3_{obs_j} \\ .. \\ Z3_{obs_e} \end{pmatrix} ; Z4_{obs,y} = \begin{pmatrix} Z4_{obs_1} \\ Z4_{obs_2} \\ Z4_{obs_j} \\ .. \\ Z4_{obs_e} \end{pmatrix} \tag{9}$$

where j is the index for the examined day of the year y (j = 1, ..., e).

The software SIC^2 can compute the values of discharge and water level along PS under two boundary conditions only in water level terms; for PS they were represented by $Z1_{obs,y}$, and $Z4_{obs,y}$. The daily simulated water level values at WL OUT_1, and WL IN_2 ($Z2_{sim,y}$ and $Z3_{sim,y}$) were compared

to those that were measured ($Z2_{obs,y}$ and $Z3_{obs,y}$) in order to demonstrate the reliability and accuracy of the hydraulic model, and therefore, of the computed discharge values. The vectors $Z2_{sim,y}$ and $Z3_{sim,y}$ can be defined as:

$$Z2_{sim,y} = \begin{pmatrix} Z2_{sim_1} \\ Z2_{sim_2} \\ Z2_{sim_j} \\ .. \\ Z2_{sim_e} \end{pmatrix} ; \ Z3_{sim,y} = \begin{pmatrix} Z3_{sim_1} \\ Z3_{sim_2} \\ Z3_{sim_j} \\ .. \\ Z3_{sim_e} \end{pmatrix} \tag{10}$$

where j is the index for the examined day of the year y (j = 1, ..., e).

The simulations can be run under steady or unsteady state. The use of the former can be justified by the slow dynamics in the CER and the time and CPU (Central Processing Unit) memory saving. In particular, SIC^2 allows implementing a series of steady state simulations. The year 2015 was examined as a first test. The hydraulic model was run under a series of one-day steady state simulations and under one-day and 10-min unsteady state simulations.

A refined hydraulic model can be obtained after an optimization process. It allows for minimizing the differences in water level terms at WL OUT_1 and WL IN_2 playing on the values of the hydraulic variables and of a scaling factor for the offtakes; they were set as parameterized variables.

The optimization process consisted in a set of parameters to be evaluated, a criterion to be minimized, and a minimization function; it was based on the dialogue between SIC^2 and Matlab$^®$ (version 9.1, The MathWorks, Inc., Natick, MA, USA).

In SIC^2, the parameterized hydraulic variables were explicit *Cd1* and *Cd2*, gate discharge coefficients of Culv_1 and Culv_2; *n*, *n1* and *n2*, Manning's coefficients along PS, within Culv_1 and Culv_2.

In Matlab$^®$, this hydraulic set was recalled and the scaling factor *Cq* allowed multiplying the offtake discharge values from Section 2.4.1. In the math code, the criterion and the minimization function were implemented.

The vectors *diff2*$_y$ and *diff3*$_y$ can be defined as:

$$diff2_y = Z2_{sim,y} - Z2_{obs,y} \qquad and \qquad diff3_y = Z3_{sim,y} - Z3_{obs,y} \tag{11}$$

Therefore, the criterion to be minimized *J* was expressed as:

$$J = \sqrt{\sum_{j=1}^{e} \left[\frac{(diff2_y)^2}{\sigma 2_y^2} + \frac{(diff3_y)^2}{\sigma 3_y^2} \right]} \tag{12}$$

where j is the index for the examined day of the year y (j = 1, ..., e), $\sigma 2_y$, and $\sigma 3_y$ are the vectors containing the weights (values of 10 or 1), indicating whether a measure is affected by errors or not.

The iterative play on the parameterized hydraulic variables influenced the elements of the vectors *diff2*$_y$ and *diff3*$_y$, and consequently, the criterion *J*.

The minimization function considered was based on the Nelder-Mead simplex direct search algorithm, already implemented in Matlab$^®$ [70]. In Figure 3, the iterations on *J* are shown for the year 2015.

At the end of the process, the minimization function identified parameterized hydraulic variables values that represent real minimum for the criterion (Figure 4).

For every year, these values were used for running the hydraulic simulations in SIC^2. The obtained model was called "optimized" and it returned the simulated discharges and water levels along PS. Finally, the optimization process was characterized by the cost of *J* that indicated the criterion value at the end of the iterations.
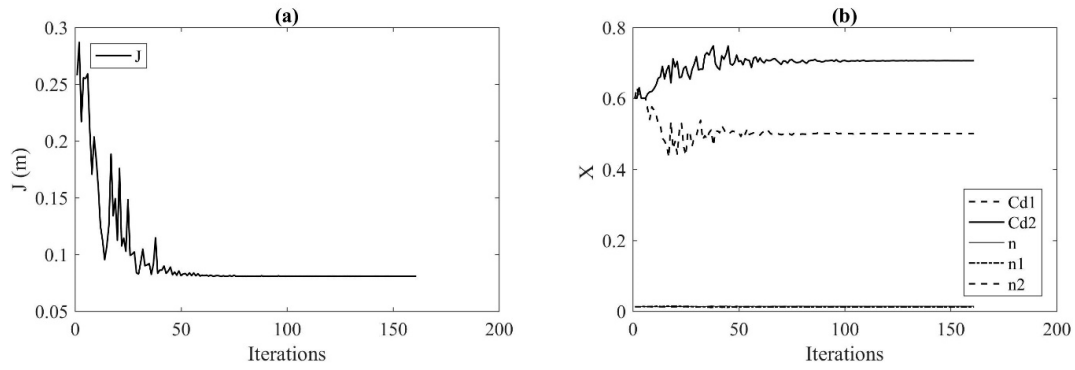
Figure 3. For 2015, the values of J (**a**) and of the parameterized hydraulic variables contained in the vector X (**b**) during the iterations of the optimization process that resulted in the minimization of the criterion.
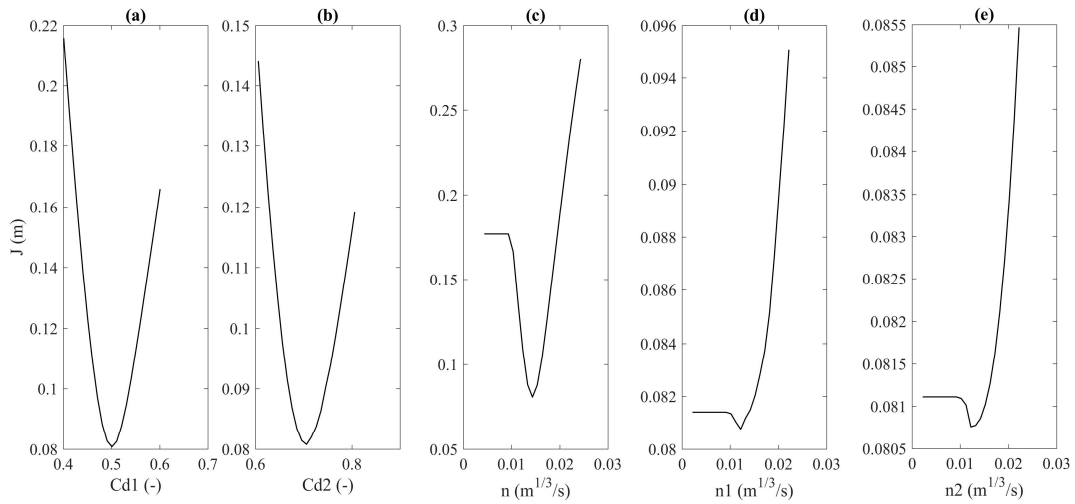

Figure 4. For 2015, *Cd1* (**a**), *Cd2* (**b**), n (**c**), *n1* (**d**), *n2* (**e**), the cuts of J around the minimum values of the parameterized hydraulic variables. In all cases they represent real minimum for the criterion.

Within the overall methodology, the measurement reliability represented a significant issue. The measures that are probably affected by errors (called "suspicious measures") can be contained in WL IN_1 and WL OUT_2 (boundary conditions), as in WL OUT_1 and WL IN_2 (optimization conditions) data series. The former affected the hydraulic model, while the latter the optimization process.

The days that are affected by suspicious measures were weighted in the optimization process through the elements of $\sigma 2_y$ and $\sigma 3_y$. In particular, if a day j is affected by a suspicious measure, the weight ($\sigma 2_j$; $\sigma 3_j$) was set as 10; otherwise, it was equal to 1.

A detection method was elaborated considering the vectors $Z1_{obs,y}$, $Z2_{obs,y}$, $Z3_{obs,y}$, $Z4_{obs,y}$, $Q2_{sim,y}$, and $Q3_{sim,y}$. The latter two contained simulated values of discharge (output of the optimized hydraulic model) at the Culv_1 and Culv_2, respectively.

They can be expressed as:

$$Q2_{sim,y} = \begin{pmatrix} Q2_{sim_1} \\ Q2_{sim_2} \\ Q2_{sim_j} \\ .. \\ Q2_{sim_e} \end{pmatrix} ; \ Q3_{sim,y} = \begin{pmatrix} Q3_{sim_1} \\ Q3_{sim_2} \\ Q3_{sim_j} \\ .. \\ Q3_{sim_e} \end{pmatrix} \tag{13}$$

where *j* is the index for the examined day of the year *y* ($j = 1, ..., e$).

The method was based on the vectors:

$$delta_y = Z2_{obs,y} - Z3_{obs,y};$$

$$delta1_y = Z1_{obs,y} - Z2_{obs,y};$$ (14)

$$delta2_y = Z3_{obs,y} - Z4_{obs,y};$$

For the day *j*, their elements represented the differences in water level terms along the segment and at the Culv_1 and Culv_2, respectively. The plots of *delta_y*-*delta1_y*, and *delta_y*-*delta2_y* were used to evaluate in which vector the suspicious measures were located. The outliers of the data linear fitting were investigated. If the element *j* of *delta_y* results as an outlier in both plots, a suspicious measure was in $Z2_{obsj}$ or in $Z3_{obsj}$. If the element *j* of *delta_y* results as an outlier in the first plot but not in the second, the suspicious measure was in $Z1_{obsj}$. If the element *j* of *delta_y* is an outlier in the second plot but not in the first, the suspicious measure was in $Z4_{obsj}$. To evaluate if a suspicious measure is in $Z2_{obsj}$ or $Z3_{obsj}$, $Q2_{sim,y}$-*delta1_y*, and $Q3_{sim,y}$-*delta2_y* were plotted. For both, a data quadratic fitting of data was considered. If the *j*-th element of *delta1_y* results as an outlier, the suspicious measure was in $Z2_{obsj}$ while if the element *j* results as an outlier of *delta2_y*, the suspicious measure was in $Z3_{obsj}$.

The most significant results obtained are given in Section 3.1.

2.5. Description of the Extended Segment (ES)

The multi-disciplinary modelling approach was then applied over a 22 km Extended Segment (ES) of the CER (Figure 5). Its downstream corresponds to WL IN_1 and its upstream is located in a delivery tank, few meters away from the pumping station Pieve di Cento exit. The latter counts seven pumps with a maximum capacity of 50 m^3/s and a maximum head of 4.5 m. For the first 33 m along the segment, the trapezium cross section top width is higher (85 m) and the bed altimetry varies from 10.79 m to 13.50 m above the sea level. Later, ES presents three different composite trapezium cross sections (top width from 26.4 m to 22.8 m; bottom width from 5.0 m to 3.3 m; side slope 3:1 and 1.5:1) and a constant slope (bed altimetry from 13.50 m to 12.81 m above the sea level). Four culverts under passing two roads (Road crossing_1 and Road crossing_2), the Navile Canal (Culv_3), and the Savena River (Culv_4) are characterized by a rectangular flow section of 36 m^2 (Figure 5). The road crossings present a modest length (about 20 m), while Culv_3 and Culv_4 are about 63 m and 86 m, respectively. The 12 occurring offtakes serve a total irrigated area of about 12,580 ha. The water gauges involved are only two at the ES extremities: WL OUT_0 (at the upstream) and WL IN_1 (at the downstream).

2.6. Application of the Multi-disciplinary Modelling Approach on ES

ES was characterized by a high complexity in geometric and functioning terms (Section 2.5). Moreover, the hydraulic data availability was poor; in fact, only two locations were equipped with water gauges. The multi-disciplinary modelling approach was applied over this segment in order to test its validity in more difficult conditions, representing a typical configuration in irrigation networks and with a significant lack of hydraulic measurements [19].

The offtake discharges decadal values were estimated as in Section 2.4.1. Due to the lack of available data, the PS flowing discharge resulted at WL OUT_1, was used to calculate the flowing discharges over ES, to run the optimized hydraulic model, and to compare the simulated and measured water level values at WL OUT_0. It was considered to be reliable due to the values of the parameterized hydraulic variables, of the linear interpolation parameters, and of the RMSE (Section 3.1.3). In particular, the PS flowing discharge values were used to define the ES upstream boundary conditions.
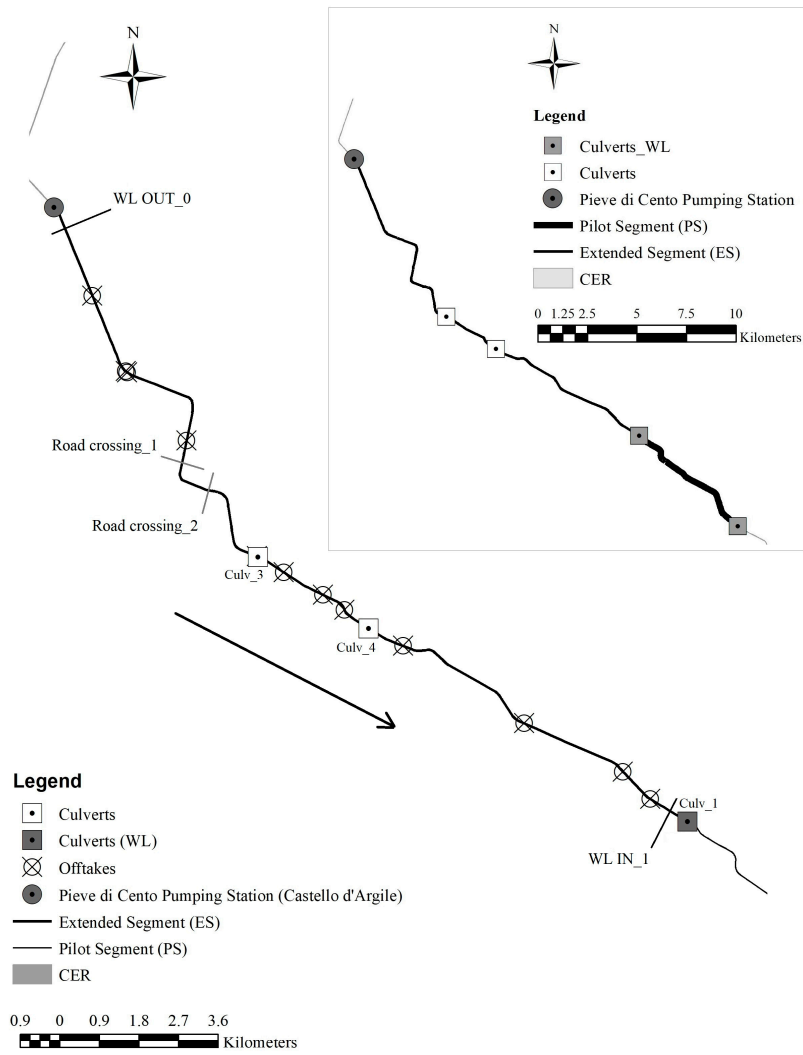
Figure 5. The scheme of ES: The 12 irrigation offtakes, the three culverts under passing the Idice River (Culv_1), the Navile Canal (Culv_3), and the Savena River (Culv_4), the two water gauges (WL OUT_0 and WL IN_1) at the OUT of the pumping station Pieve di Cento and at the IN of Culv_1, the two road crossings.

For the year y, the vector containing the calculated discharge values of a generic offtake k (Section 2.4.1) can be expressed as:

$$q_{kC,y} = \begin{pmatrix} q_{kCn_1} \\ q_{kCn_2} \\ q_{kCn_j} \\ .. \\ q_{kCn_e} \end{pmatrix} \tag{15}$$

where j is the index for the examined day of the year y ($j = 1, ..., e$).

Defining as $q_{totC,y}$, the total offtake discharges vector:

$$q_{totC,y} = \begin{pmatrix} q_{totC_1} \\ q_{totC_2} \\ q_{totC_j} \\ .. \\ q_{totC_e} \end{pmatrix} \tag{16}$$

Its element q_{totCj} was calculated as:

$$q_{totC_j} = \sum_{k=1}^{12} q_{kCn_j} \tag{17}$$

where k is the index of the generic offtake ($k = 1, \ldots, 12$).

For the year y, the vector $Q0_y$ represented the ES upstream boundary conditions. It was obtained as:

$$Q0_y = Q2_{sim,y} + q_{totC,y} \tag{18}$$

whereas, the $Z1_{obs,y}$ values reported were used as the downstream boundary conditions. The hydraulic model was implemented under a series of one-day steady state simulations. For every year, the vector $Z0_{obs,y}$ contains the daily measured water levels values at WL OUT_0. They were used for testing the model performances and for evaluating the optimization process. $Z0_{obs,y}$ can be defined as:

$$Z0_{obs,y} = \begin{pmatrix} Z0_{obs_1} \\ Z0_{obs_2} \\ Z0_{obs_j} \\ .. \\ Z0_{obs_e} \end{pmatrix} \tag{19}$$

where j is the index for the examined day of the year y ($j = 1, ..., e$).

The optimized parameterized hydraulic variables set was larger than that of PS. It consisted in $Cd3$, $Cd4$, $Cd5$, and $Cd6$, gate discharge coefficients of Culv_3 and Culv_4 and of the two road crossings; n, $n3$, $n4$, $n5$, and $n6$, Manning's coefficients along ES, within the two culverts and the two road crossings. The significant uncertainty that affects the measured water levels at WL OUT_0 (Section 2.2) was reflected in the larger parameterized hydraulic variables set size. The high degree of freedom allowed for obtaining physically possible values of the parameters and the lower cost of J at the optimization process end. The gate discharge coefficients values could not be imposed as those of PS because the geometric and functioning characterization difference. Moreover, if the Manning's coefficients are imposed, the optimization process gives higher gate discharge coefficients values (>1) that are not physically correct. The offtake discharges scaling factor was not considered, as explained in Section 3.1.3.

For the year y, the vector $Z0_{sim,y}$ contained the daily simulated water levels at WL OUT_0:

$$Z0_{sim,y} = \begin{pmatrix} Z0_{sim_1} \\ Z0_{sim_2} \\ Z0_{sim_j} \\ .. \\ Z0_{sim_e} \end{pmatrix} \tag{20}$$

where j is the index for the examined day of the year y ($j = 1, ..., e$).

The optimization criterion was based on the definition of the vectors $diff0_y$ and $\sigma0_y$. The former contained the values of the daily differences between simulated and measured water levels at WL OUT_0, as:

$$diff0_y = Z0_{obs,y} - Z0_{sim,y} \tag{21}$$

The vector $\sigma0_y$ weighted the measures probably affected by errors ("suspicious") located in $Z0_{obs,y}$. The detection involved the Pieve di Cento pumps functioning data. In particular, for the year y,

the vectors $Z0_{pmax,y}$ and $Z0_{pmin,y}$ contained the daily maximum and minimum values of the delivery tank water level that is registered by the pumps functioning, as:

$$Z0_{pmax,y} = \begin{pmatrix} Z0_{pmax_1} \\ Z0_{pmax_2} \\ Z0_{pmax_j} \\ .. \\ Z0_{pmax_e} \end{pmatrix} ; \; Z0_{pmin,y} = \begin{pmatrix} Z0_{pmin_1} \\ Z0_{pmin_2} \\ Z0_{pmin_j} \\ .. \\ Z0_{pmin_e} \end{pmatrix} \tag{22}$$

where j is the index for the examined day of the year y ($j = 1, ..., e$).

For every day j, the functioning range $Z0_{pmaxj}$-$Z0_{pminj}$ was identified. If $Z0_{obsj}$ do not belong to it, it is defined as a suspicious measure.

The expression of the criterion J was:

$$J = \sqrt{\sum_{j=1}^{e} \frac{\left(diff0_y\right)^2}{\sigma 0_y^2}} \tag{23}$$

The minimization function is that of PS (Nelder-Mead simplex direct search algorithm).

The most significant results obtained are given in Section 3.2.

3. Results and Discussion

3.1. Pilot Segment (PS)

3.1.1. Unmeasured Offtake Discharges

For every year, the values of w_{kDm}, w_{kTn}, and w_{kCn} were calculated, as in Section 2.4.1. Out of these weights, the first one resulted generally higher than the second one; the V_{rDm}-V_{kDm}, in fact, differed considerably from V_{rTn}-V_{kTn}. When considering the year 2015 as an example, the maximum values were 23.04×10^4 m^3 and 13.68×10^4 m^3, respectively. For the same year, Figure 6a underlines the monthly variability of w_{kDm} as compared to the decadal one of w_{kTn} for two offtakes: Offtake$_1$ (reference offtake) and Offtake$_5$ (Figure 2). The weights w_{kCn} were obtained averaging *D*-data and *T*-data according to Equation (3), and they were reported in Figure 6b. The averaging of those values was needed to minimize the possible measurement errors in *D*-data, and also, to take into account that *CWR* from IRRINET are "optimal requirements", when considering that water was always fully available.
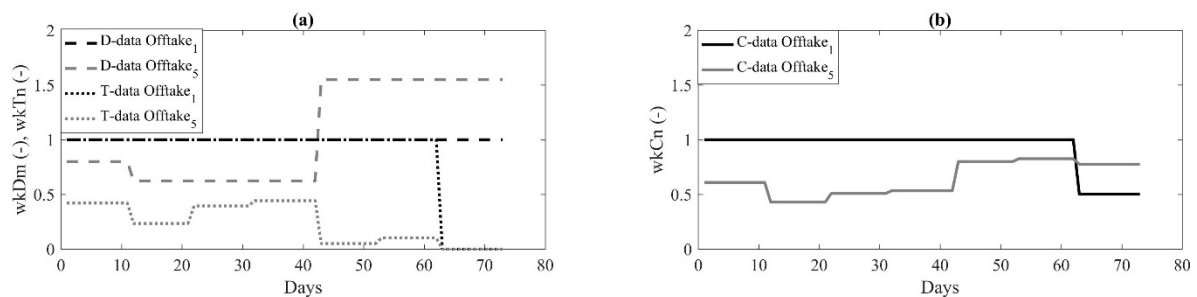

Figure 6. For the year 2015, the values of the weights w_{kDm} and w_{kTn} (**a**) and w_{kCn} (**b**) for the reference offtake (Offtake$_1$) and for a generic one (Offtake$_5$).

Over the four years of analysis, the trend of the offtake discharge values (q_{kCn}) was mainly coherent with the yearly meteo-climatic conditions (i.e., average daily rainfall). The reference offtake

discharge values ranged from 0 m^3/s to 0.24 m^3/s. q_{kCn} of all other offtakes varied from 0 m^3/s to 0.17 m^3/s.

Figures 7a and 7b show that the two offtakes (Offtake$_1$ and Offtake$_5$) had the lowest values in 2014 (mean values of 0.021 m^3/s and 0.032 m^3/s, respectively) and the highest mainly in 2012 (mean values of 0.137 m^3/s and 0.082 m^3/s, respectively). If the month of July is considered, the discharge values of the reference offtake were lower in 2012 than in 2013 and 2015. This can be explained not only by meteo-climatic conditions (that resulted in crop stress), but also by insufficient machine, manpower, or energy availability at the field. Moreover, among the years that were analysed, the cultivated crops differ.
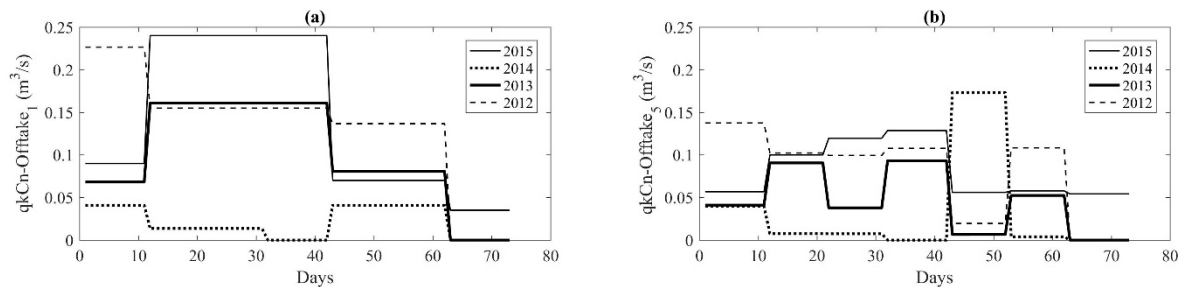

Figure 7. For every year, the variability of the diverted discharges for the reference offtake (Offatake$_1$) (**a**) and for a generic offtake (Offtake$_5$) (**b**).

3.1.2. Steady State Flow Condition

To evaluate if the hydraulic models should be run under steady or unsteady state conditions, the results of the year 2015 were analysed. They consisted in discharge and water level values at WL OUT_1 and WL IN_2. The hydraulic model of PS was run under a series of one-day steady state (Steady-1d) simulations, and under one-day (Unsteady-1d), and 10-min (Unsteady-10mn) unsteady state simulations.

The vectors *Z2sim-2015* and *Z3sim-2015* for Steady-1d and Unsteady-1d were completely overlaid. The differences obtained by comparing these vectors for Steady-1d and Unsteady-10mn reported mean values of 0.285 m and 5.347×10^{-4} m, respectively.

For Steady-1d and Unsteady-1d the vectors *Q2sim-2015* and *Q3sim-2015*, so as the simulated water levels, were completely overlaid. If the simulations of steady state and those of unsteady state with time step 10 min are compared, the resulted maximum and mean differences were 3.843 m^3/s and 0.279 m^3/s, respectively.

For the optimization of the hydraulic model, the results in water level and discharge terms can be considered to be approximatively identical for the three flow conditions that are considered.

The series of one-day steady simulations was adopted for running the hydraulic models of both PS and ES. This assumption was justified by the slow dynamics occurring in the CER, and it is also coherent with the time scale of calculated offtake discharges (decadal) and of measured water level (daily) data. The use of steady state saves time and CPU memory that is an important point, since this hydraulic calculation is embodied into an optimization loop. Using only one run, SIC^2 computes 73 steady state simulations; one for every day of the irrigation period. The hydraulic variables on a daily basis are not function of time.

3.1.3. PS optimized Model

The optimized hydraulic model returned the flowing discharges along the PS. For example, in Figure 8, the $Q2_{sim,y}$ values are reported (values at the upstream of PS). For every year, they are grouped into two vectors: $Q2_{simc}$ (output from measured water levels not affected by errors) and $Q2_{sims}$ (output from measured water levels probably affected by errors, Section 2.4.2).

The lowest values of flowing discharge were calculated for the rainier year (2014) and they were 17.560 m^3/s ($Q2_{sim,2014}$) and 16.660 m^3/s ($Q3_{sim,2014}$), with standard deviations of 2.694 m^3/s and 3.204 m^3/s, respectively. When considering $Q2_{sim,y}$ as an example, the years 2013 and 2015 were characterized by higher flowing discharge mean values (23.930 m^3/s and 21.710 m^3/s) and standard deviation values (4.230 m^3/s and 4.841 m^3/s) as compared to those of the year 2012 (20.700 m^3/s and 2.538 m^3/s, respectively). This can be justified by the limiting factors that are mentioned in Section 3.1.1. Therefore, the years with extreme climatic conditions (2014 and 2012) presented less variability in relation to flowing discharge mean values when compared to the years 2013 and 2015 characterized by the alternation of dry and rainy intervals.

The values of the flowing discharge were the result of many factors: offtake discharges (that followed characterization, as explained in Section 3.1.1), the modelled functioning of culverts and the measured water levels.
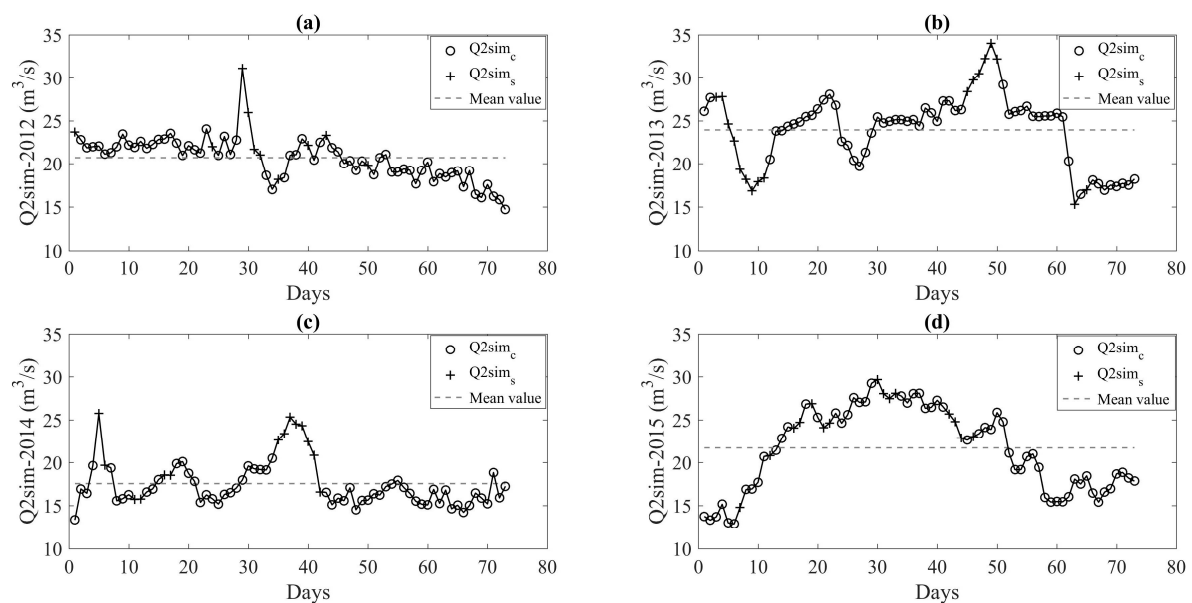

Figure 8. For every year: 2012 (**a**); 2013 (**b**); 2014 (**c**) and 2015 (**d**), the values of $Q2_{sim}$ obtained from the optimized model.

For the year y, the optimized hydraulic model performances were evaluated through the values of the parameterized variables and of the differences between water levels simulated and measured at WL OUT_1 and WL IN_2. At the end of the optimization process, the values of the hydraulic variables should be physically correct and coherent with literature [68].

For Cq, the yearly values that were obtained resulted close to 1. If the optimization process were cut around these values, they would not represent real minimum. The offtake discharges impact on the water levels at WL OUT_1 and WL IN_2 around their nominal values was less than the measurement accuracy considered (±0.05 m); the offtake discharges represented small rates if compared to flowing discharges. When considering the year 2015 as an example, the flowing discharge maximum and minimum values were 29.66 m^3/s and 12.88 m^3/s, respectively, while the reference offtake discharge ranged from 0.24 m^3/s (0.81% of the flowing discharge maximum) to 0.07 m^3/s (0.24% of the flowing discharge minimum). Cq cannot be considered as one of the parameters for the optimization process since it did not have any influence on it.

The parameterized hydraulic variables and the cost of the criterion are reported in Table 3 for every year of analysis. The results that were obtained with the suspicious measures weights are discussed in the following paragraphs.

Table 3. The values of the five parameterized variables and the cost of the criterion obtained from the optimization process: Without (above) and with the weights of suspicious measures (below).

Year	Parameterized Hydraulic Variables					Cost of the Criterion
	Cd1 (-)	*Cd2* (-)	*n* (m$^{1/3}$/s)	*n1* (m$^{1/3}$/s)	*n2* (m$^{1/3}$/s)	*J Cost* (m)
	Without Suspicious Measures Weights					
2012	0.37	0.64	0.014	0.015	0.015	0.1742
2013	0.68	0.76	0.015	0.009	0.011	0.2799
2014	0.39	0.82	0.016	0.015	0.008	0.2331
2015	0.49	0.69	0.015	0.012	0.013	0.1036
	With Suspicious Measures Weights					
2012	0.37	0.65	0.014	0.014	0.015	0.1460
2013	0.71	0.74	0.016	0.009	0.011	0.1480
2014	0.44	0.80	0.015	0.013	0.010	0.1101
2015	0.50	0.71	0.014	0.012	0.012	0.0808

The gate discharge coefficients (*Cd1* and *Cd2*) refer to submerged flow for both culverts. The *Cd2* values were coherent with the range 0.60–0.85 that was reported in literature [69,71–73]. For all years, surface flow occurred within Culv_2. For some years, the *Cd1* values significantly differed from the literature range, and it can be explained by applying Equation (8) to the two gates at Culv_1 and Culv_2. For example, when Equation (8) was applied on the year 2012 (*Cd1* = 0.37, *Cd2* = 0.64), for Culv_1, the term (Z_{up}-Z_{dn}) reported maximum and minimum values of 0.13 m and 0.03 m, respectively. They were higher than those at Culv_2 that were 0.07 m and 0.01 m, respectively. Due to the modest impact of the offtakes, the values of the discharges at the two culverts were similar, and therefore the gate discharge coefficient at Culv_1 has to be lower than the one at Culv_2. Within Culv_1, both flow types (surface and piped) occurred. The years 2012 and 2015 were characterized by 39 days of surface and 34 days of piped flows. The years 2013 and 2014, on the other hand, presented mainly surface flow (57 and 59 days, respectively).

The *n* values that were obtained were coherent with the reported literature range for concrete canals (0.010–0.020 m$^{1/3}$/s) [68]. Over the last four years, the mean value was 0.0147 m$^{1/3}$/s and the maximum difference attested was 0.002 m$^{1/3}$/s (2012–2013). The *n1* and *n2* values were coherent with the literature range for concrete culverts (0.010–0.014 m$^{1/3}$/s) [74] and both had a mean of 0.012 m$^{1/3}$/s. When considering the analysis period, the maximum difference among the years was 0.005 m$^{1/3}$/s (between 2012 and 2013 for *n1*, and between 2012 and 2014 for *n2*). The Manning's coefficient is the result of many factors: Basic value (roughness of the material that was used to line the canal), irregularities of the canal bed, cross sections variations, obstacles, vegetation growth, and meandering [75,76]. Along the PS, the Manning's coefficient was stable; its variations can be related to the presence of obstacles (debris, downed plants, and dropped obstacles) and algae growth. For the culverts, it showed more variability and it was the result of many possible factors, such as the grids at the culverts entrances, which involve head losses, the gates modelling approximations, and the additional head losses due to the change of geometry between open and closed flow cross sections.

For every year, the performances of the optimized hydraulic model were evaluated through the elements contained in $Z2_{sim,y}$ and $Z3_{sim,y}$ (Figure 9).

The differences between simulated and measured water levels at WL OUT_1 and at WL IN_2 affected the cost of the criterion and the linear interpolation parameters. The former was also influenced by the $\sigma2_y$ and $\sigma3_y$ vectors, as shown in Table 3. The maximum difference for the cost of the criterion was 0.1319 m (0.2799–0.1480 m) for 2013.

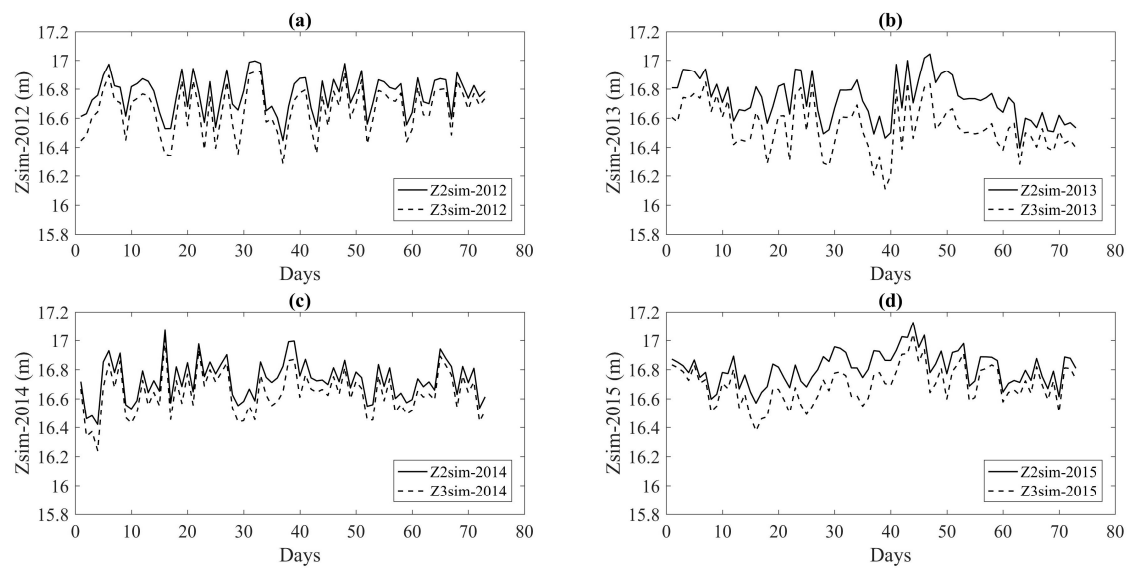**Figure 9.** For every year: 2012 (**a**); 2013 (**b**); 2014 (**c**) and 2015 (**d**), the simulated water level values contained in $Z2_{sim}$ and $Z3_{sim}$.

For every year, in order to compare simulated and observed water level values, the former were plotted in the X-axis, while the latter in the Y-axis [77–81]. In this plot format, the points on the Y = X line represent the perfect correspondence between model-predicted and measured values; therefore, the intercept and the slope are 0 and 1, respectively [82]. Points below or above that line indicate over or under-estimations of the model [77]. In Figure 10, the elements of the vector $Z2_{sim,y}$ were plotted versus those of the vector $Z2_{obs,y}$. The former were reported for optimized (Opt) and non-optimized (Non-Opt) models.
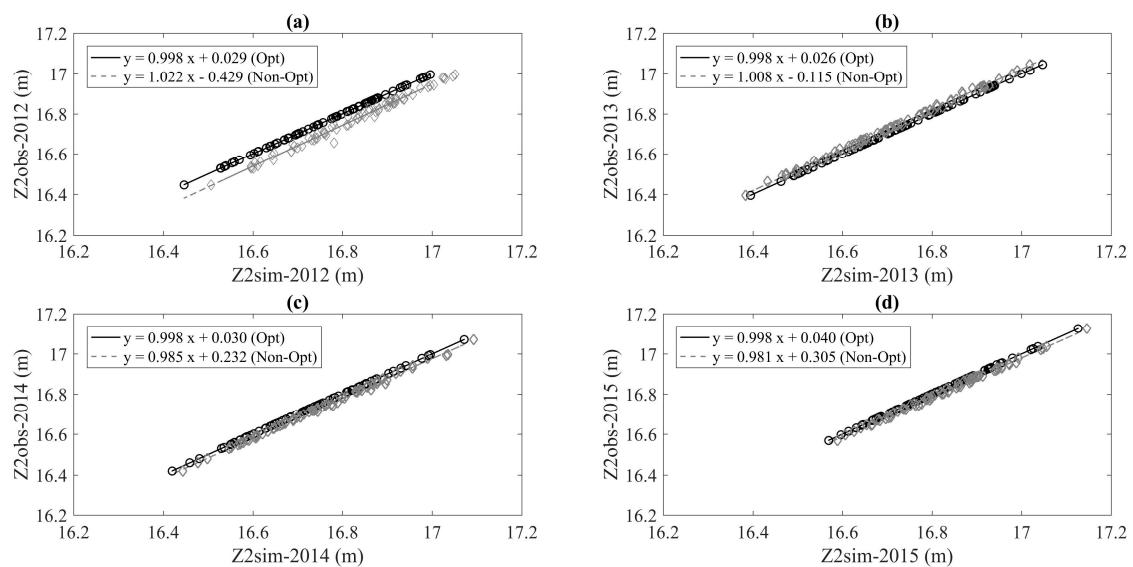

Figure 10. For every year: 2012 (**a**); 2013 (**b**); 2014 (**c**) and 2015 (**d**), the linear interpolation of $Z2_{obs}$ and $Z2_{sim}$ for both optimized and non-optimized models.

The validity of the optimized model was verified because of the line interpolation parameters values were closer to the optimum ones, especially in line intercept terms (i.e., 0.029 instead of 0.429 for *Z2sim-2012*). Over the four years, the mean values of intercept and slope line were 0.031 and 0.998, respectively. The same evaluation method was applied to $Z3_{sim,y}$ and $Z3_{obs,y}$ (Figure 11). Also, in this

case, the optimized model shows an excellent fit, reporting mean values of intercept and slope line of 0.105 and 0.994, respectively.
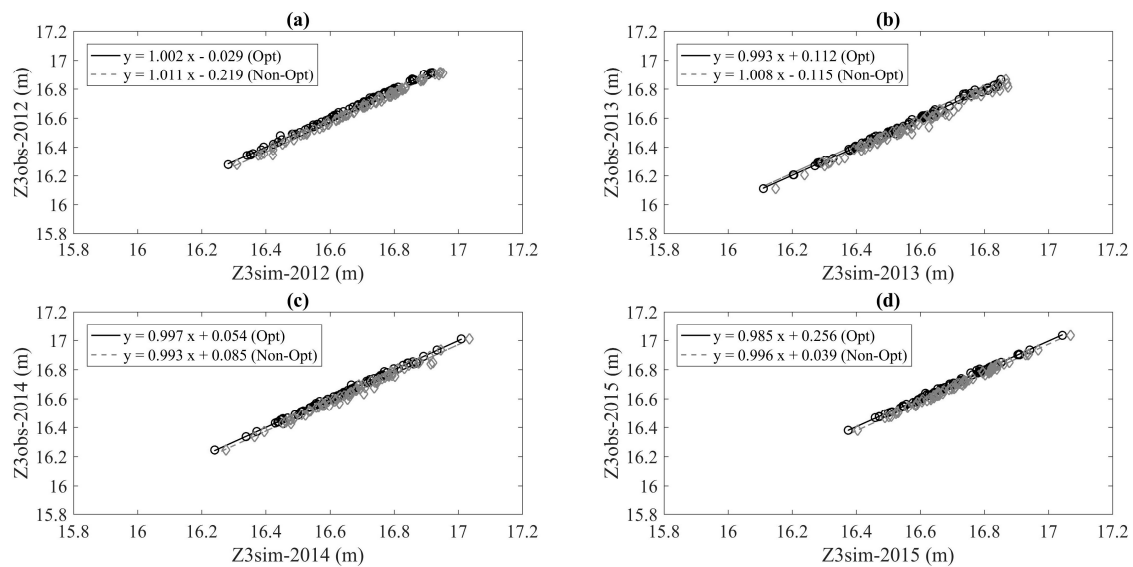

Figure 11. For every year: 2012 (**a**); 2013 (**b**); 2014 (**c**) and 2015 (**d**), the linear interpolation of $Z3_{obs}$ and $Z3_{sim}$ for both optimized and non-optimized models.

The performances of the optimization process have been also evaluated in terms of the root mean square error (RMSE) (Table 4). For the optimized model, the RMSE was calculated at WL OUT_1 and at WL IN_2 reporting mean values of 4.661×10^{-4} m and 8.150×10^{-3} m, respectively. They significantly differ from those of the non-optimized one (mean value of 0.0302 m at WL OUT_1 and 0.0285 m at WL IN_2).

Table 4. The root mean square error (RMSE) values for both optimized and non-optimized models at WL OUT_1 and WL IN_2.

Year	RMSE (m)	
	Non-Optimized Hydraulic Model	**Optimized Hydraulic Model**
WL OUT_1		
2012	0.0586	2.9×10^{-4}
2013	0.0220	6.1×10^{-4}
2014	0.0216	5.8×10^{-4}
2015	0.0185	3.9×10^{-4}
WL IN_2		
2012	0.0318	6.1×10^{-3}
2013	0.0340	11.2×10^{-3}
2014	0.0316	8.3×10^{-3}
2015	0.0265	7.0×10^{-3}

Overall, the comparison among simulations highlighted the fact that the optimized model achieved excellent results, which are very close to the measured values. In the RMSE terms, the differences between the two models (non-optimized vs optimized) had maximum value of 0.0583 m, that was recorded at WL OUT_1 for the dry year (2012). Moreover, the mean differences were 0.0297 m and 0.0228 m at WL OUT_1 and WL IN_2, respectively. When considering the measurements accuracy order of magnitude (± 0.05 m), the optimization process significantly improved the obtained results.

3.2. Extended Segment (ES)

The ES offtake discharges were calculated as in Section 2.4.1, and the q_{kCn} obtained were mainly coherent with the yearly meteo-climatic condition. In particular, the ES reference offtake reported minimum (0.02 m³/s) and maximum (1.17 m³/s) values during the rainy and the dry years, respectively. Moreover, q_{kCn} for all other offtakes varied from 0 m³/s (2014) to 0.87 m³/s (2012). This range was larger than those of PS (0–0.24 m³/s for the reference offtake and 0–0.17 m³/s for all other offtakes). In fact, the ES irrigated land supplied is 1.5 times larger (12,580 ha) than that of PS.

At WL OUT_0, the flowing discharges calculated with the Equation (18) are reported in Figure 12. For every year, the *Q0* elements were grouped in *Q0_s* and *Q0_c* vectors in order to distinguish the flowing discharge values that are based on *Q2_sims* and *Q2_simc*, respectively.
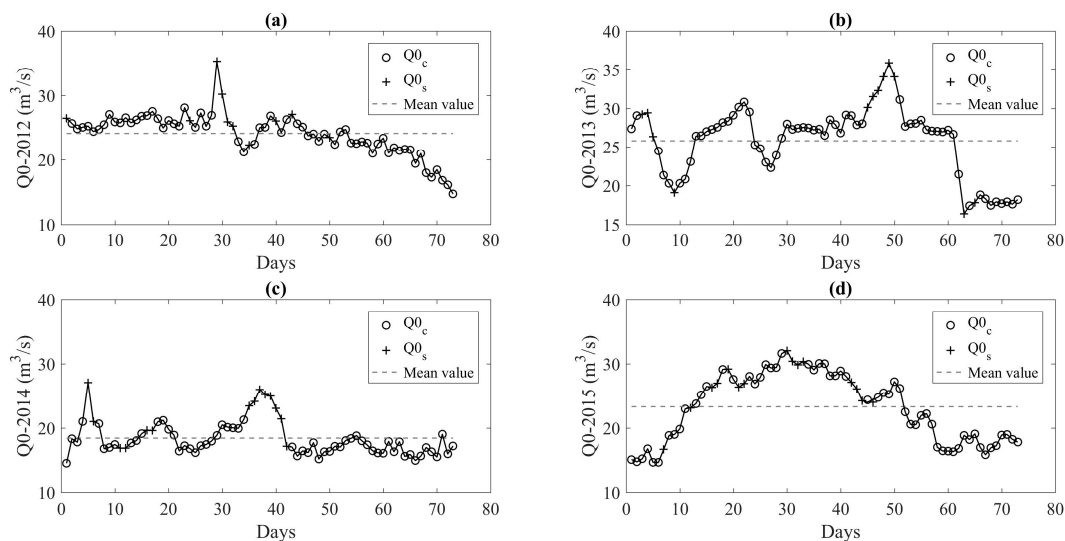

Figure 12. For every year: 2012 (**a**); 2013 (**b**), 2014 (**c**) and 2015 (**d**), the values of discharge (*Q0*) calculated at WL OUT_0.

The lowest values of flowing discharges resulted for the rainy year with a mean value of 18.46 m³/s (standard deviation of 2.70 m³/s); the highest values were related to 2012 (24.13 m³/s on average with a standard deviation of 3.22 m³/s) and 2013 (25.81 m³/s on average, standard deviation of 4.569 m³/s).

For the year *y*, the performances of the ES optimized hydraulic model were evaluated through the values of the parameterized hydraulic variables and the differences between simulated and measured water levels at WL OUT_0. When considering the hydraulic variables, the optimization process returned physically possible values while only using a larger set of parameters. In particular, four gate discharge coefficients and five Manning's coefficients were investigated to characterize ES (in roughness terms) and every culvert (in roughness and head loss terms). For three years, the values of the parameterized hydraulic variables obtained are reported in Table 5.

Table 5. The values of the nine parameterized variables and of the cost of the criterion obtained from the optimization process.

Year	Parameterized Hydraulic Variables									Cost of the Criterion
	Cd3 (-)	*Cd4* (-)	*Cd5* (-)	*Cd6* (-)	*n* (m$^{1/3}$/s)	*n3* (m$^{1/3}$/s)	*n4* (m$^{1/3}$/s)	*n5* (m$^{1/3}$/s)	*n6* (m$^{1/3}$/s)	*J* Cost (m)
2012	0.60	0.45	0.62	0.52	0.020	0.020	0.013	0.011	0.010	0.5057
2013	0.58	0.60	0.58	0.58	0.014	0.013	0.013	0.013	0.013	0.4667
2015	0.42	0.59	0.43	0.45	0.011	0.019	0.019	0.019	0.010	0.3465

For every year of analysis, the optimization process was run in order to obtain the parameterized hydraulic variables values. For the year 2014, it could not end and it tended to minimized the criteria assigning negative values to the Manning's coefficients and high values (>1) to the gate discharge coefficients. So, for this year, the optimization loop was not finalized.

All gate discharge coefficients referred to submerged flow. The values obtained presented less variability than those of PS (Table 3). They were around 0.60, except for the year 2015 (mean value of 0.47). In 2012, the four culverts were mainly characterized by piped flow (as for Culv_2 of PS), while the year 2013, except for Culv_4, presented mainly free flow conditions.

As for PS, the *n* values that were obtained were coherent with the literature range reported for concrete canals 0.010–0.020 m$^{1/3}$/s [68]. Over the three years, the mean value was 0.015 m$^{1/3}$/s (very similar to PS *n*) and the maximum difference of 0.009 m$^{1/3}$/s was between the years 2012 and 2015 (0.002 m$^{1/3}$/s in PS). The *n3*, *n4*, *n5* and *n6* values were coherent with the range 0.010–0.014 m$^{1/3}$/s for concrete culverts [74], except for the year 2015, for which the values were higher (0.019 m$^{1/3}$/s maximum). As said before, the Manning's coefficient differences can be attributed to several factors, such as geometric irregularities or variations of the canal bed and of cross sections, obstacles, vegetation growth, and meandering. Moreover, the field survey estimated the accuracy of $Z0_{obs,y}$ values (±0.10 m) to be lower than those in PS.

When considering the same year *y*, the ES *J* cost quite significantly differed from PS, and the values of the elements contained in *diff2$_y$*, *diff3$_y$* and *diff0$_y$* can justify these results. In fact, considering the year 2015 as an example, the maximum absolute values (only for days not affected by suspicious measures) are 0.015 m at WL OUT_1 (*diff2$_y$*) and 0.011 m at WL IN_2 (*diff3$_y$*), while at WL OUT_0 (*diff0$_y$*), it was much higher and very close to the accuracy threshold (0.102 m). In any case, Figure 13 shows that all the single elements of $Z0_{sim,y}$ are within the $Z0_{obs,y}$ accuracy range (±0.10 m), except for few days (eight for 2012, nine for 2013, and two for 2015) that are related to $Z0_{obsj}$ or $Q2_{simj}$ and that were probably affected by errors.
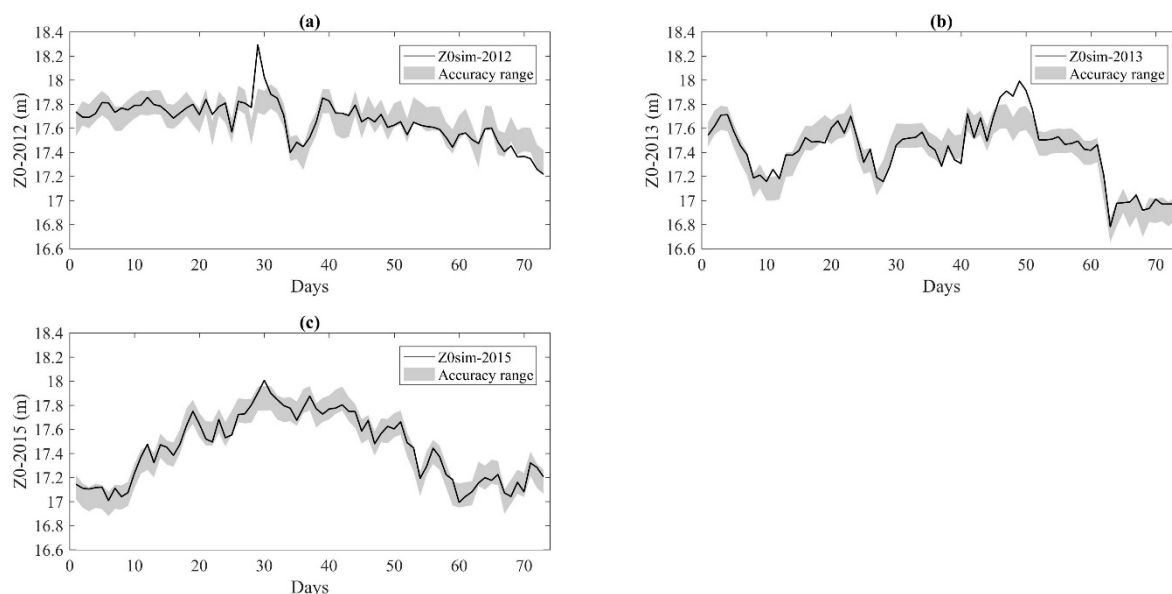

Figure 13. The simulated water level values contained in $Z0_{sim}$ for the years 2012 (**a**), 2013 (**b**) and 2015 (**c**).

As for PS, the vectors $Z0_{sim,y}$ and $Z0_{obs,y}$ were plotted (Figure 14) in order to detect the modelling impacts of the *diff0$_y$* elements. The intercept and the slope of the linear correlation were evaluated, and they were compared with the optimum values (i.e., perfect fitting) and with those reported for PS.
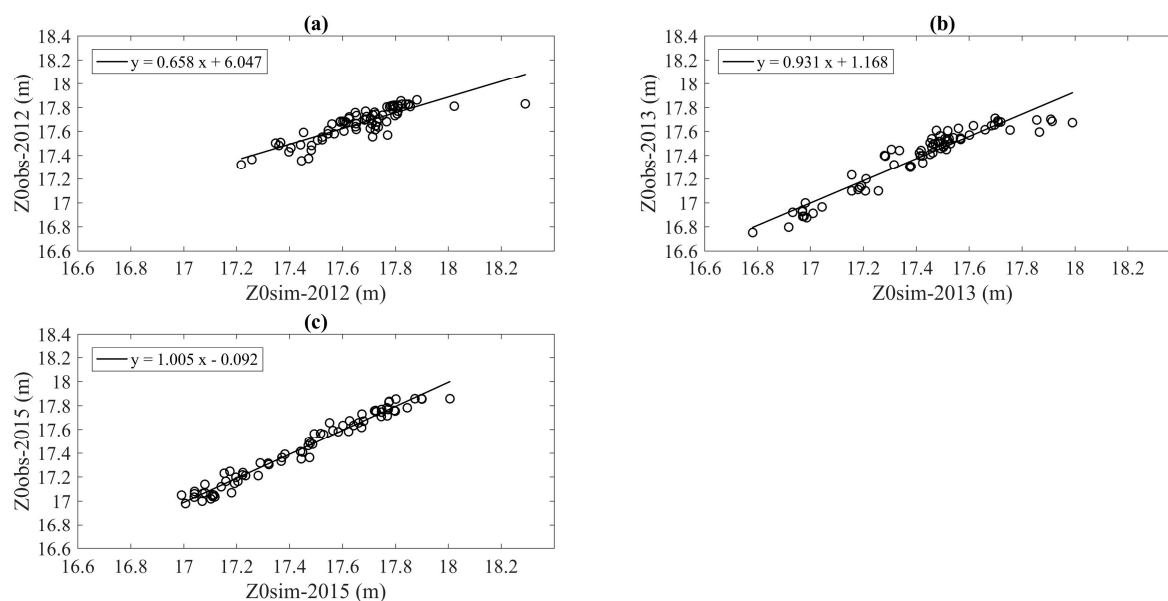
Figure 14. The linear interpolation of $Z0_{obs}$ and $Z0_{sim}$ for the optimized model for the years 2012 (**a**), 2013 (**b**) and 2015 (**c**).

The results can be considered excellent for the years 2013 and 2015, with RMSE values of 0.09 m and 0.05 m, respectively. For 2012, especially the intercept of the linear interpolation (6.047) was significantly different from the optimal value (0). As already reported by Mesplé [83], the modelling overestimation/underestimation was probably combined with the proportionality of the gap between the measured and simulated values. Therefore, the RMSE for 2012 (0.09 m) was similar to the other years.

Overall, the RMSE values in ES simulations were higher than those reported in PS, indicating that the model worked better in a segment that was characterized by simpler geometry and with higher availability and reliability of measured hydraulic data. When the model was tested on a more complex reality i.e., ES, it had to face two critical aspects: A scarce number and a lower accuracy of the hydraulic measured data. The latter affected the optimization process, especially for the years with extreme climatic conditions. In fact, the dry 2012 was characterized by an intense functioning of pumps with a maximum daily difference in water level terms of 1.23 m. On the contrary, the rainy 2014 presented lower irrigation demands and therefore the functioning of pumps was more intermittent. This implies that, due to the slope of ES (3.8×10^{-5}), a backwater flow occurred affecting the optimization process and leading to a poor representation of the reality. The multi-disciplinary modelling approach developed in this study presented satisfying results for the two remaining years (2013 and 2015).

4. Conclusions

A low availability of hydraulic data can seriously affect efficient management of irrigation canals. Therefore, this paper presents a novel approach that can be applied to reconstruct the missing hydraulic data by combining hydraulic modelling and an irrigation DSS (that was developed at a regional scale).

The approach was developed on a Northern Italian canal, more specifically, on its 7 km long segment (PS), which is characterized by a quite simple geometry and full availability of water levels, and it gave very good results. Its application on a more complex segment (ES) with a poor data availability and accuracy, confirmed that the approach can be successfully used to reconstruct data for years with standard meteo-climatic conditions, while years with extreme climatic conditions are more difficult to be simulated. It was found that the measuring point and consequently instrument accuracy are key factors for obtaining a model that can well represent the reality.

Moreover, the results showed that the offtake discharges can be estimated on the base of crop water delivery schedules and combining them with measured water levels could enable calculating the discharges that are flowing through the use of an optimized hydraulic model.

However, this approach was developed on a lined concrete canal. Therefore, its application on secondary channels, often on earth with considerable infiltration losses, have to be further studied in order to optimize the hydraulic model and to increase its relevance.

Since the approach proposed allows quantifying discharges and water levels along an irrigation canal, it can be integrated with water qualitative analysis (e.g., microbiological aspects), thus widening its multi-disciplinarity.

Author Contributions: Conceptualization, M.L., P.-O.M., A.B. and A.T.; Methodology, M.L., P.-O.M., A.B. and V.D.F.; Validation, M.L., P.-O.M., A.B. and A.T.; Formal Analysis, M.L. and V.D.F.; Investigation, M.L.; Resources, P.-O.M. and A.B.; Data Curation, M.L., P.-O.M. and A.B.; Writing-Original Draft Preparation, M.L. and P.-O.M.; Writing-Review & Editing, M.L., P.-O.M., A.B. and A.T.; Visualization, M.L.; Supervision, A.T.; Project Administration, A.T.; Funding Acquisition, A.T.

Conflicts of Interest: The authors declare no conflict of interest.

Abbreviations

The following abbreviations are used in this manuscript.

Along the CER

Culv_1, Culv_2	Culverts of Pilot Segment passing under rivers
Culv_3, Culv_4	Culverts of Extended Segment passing under rivers
ES	Extended Segment
PS	Pilot Segment
WL OUT_0	Water gauge at the exit of the pumping station Pieve di Cento
WL IN_1	Water gauge at the entrance of Culv_1
WL OUT_1	Water gauge at the exit of Culv_1
WL IN_2	Water gauge at the entrance of Culv_2
WL OUT_2	Water gauge at the exit of Culv_2

Measured data

$Z0_{obs,y}$	Vector containing daily water levels at WL OUT_0 for the year y
$Z0_{pmax,y}$	Vector containing maximum daily water levels from the functioning of Pieve di Cento pumps
$Z0_{pmin,y}$	Vector containing minimum daily water levels from the functioning of Pieve di Cento pumps
$Z1_{obs,y}$	Vector containing daily water levels at WL IN_1 for the year y
$Z2_{obs,y}$	Vector containing daily water levels at WL OUT_1 for the year y
$Z3_{obs,y}$	Vector containing daily water levels at WL IN_2 for the year y
$Z4_{obs,y}$	Vector containing daily water levels at WL OUT_2 for the year y

Offtakes

Ai	Irrigable area; area covered by the crop i
C-data	Calculated data
CWR_i	Decadal cumulated optimum crop water requirement for the crop i
D-data	Declared data provided by the Associated Consortia
D_m	Duration of the month m
ED	Coefficient of the efficiency of the delivery system CER-irrigable area
EI_i	Coefficient of the efficiency of the irrigation method of the crop i
II_i	Coefficient of irrigation intensity of the crop i
q_{kCn}	Calculated discharge exiting from the offtake k during the decade n
$q_{kC,y}$	Vector containing daily calculated discharge values of the offtake k for the year y
q_{rDm}	Discharge value exiting from the reference offtake during the month m
$q_{totC,y}$	Vector containing daily calculated offtake discharges from the segment (i.e., ES) for the year y
T-data	Estimated data provided by IRRINET
V_{kDm}	Monthly cumulated volume of the offtake k from *D-data*

V_{kTn}	Decadal cumulated volume of the offtake k from *T-data*
V_{rDm}	Monthly cumulated volume of the reference offtake from the *D-data*
V_{rTn}	Decadal cumulated volume of the reference offtake from the *T-data*
w_{kCn}	Weight of the offtake k during the decade n
w_{kDm}	Weight of the offtake k during the month m from *D-data*
w_{kTn}	Weight of the offtake k during the decade n from *T-data*
Optimization	
Cd1, Cd2	Gate discharge coefficients at the entrances of Culv_1 and Culv_2
Cd3, Cd4	Gate discharge coefficients at the entrances of Culv_3 and Culv_4
Cd5, Cd6	Gate discharge coefficients at the entrances of 2 road crossings (ES)
Cq	Scaling factor of the offtake discharges
J	Criteria to be minimized
n	Manning's coefficient on the CER open-flow sections (along PS or ES)
n1, n2	Manning's coefficients within Culv_1 and Culv_2
n3, n4	Manning's coefficients within Culv_3 and Culv_4
n5, n6	Manning's coefficients within the 2 road crossings
$Q0_y$	Vector containing daily calculated flowing discharges at WL OUT_0 for the year y
$Q2_{sim,y}$	Vector containing daily simulated flowing discharges at WL OUT_1 for the year y
$Q3_{sim,y}$	Vector containing daily simulated flowing discharges at WL IN_2 for the year y
$Z0_{sim,y}$	Vector containing daily simulated water levels at WL OUT_0 for the year y
$Z2_{sim,y}$	Vector containing daily simulated water levels at WL OUT_1 for the year y
$Z3_{sim,y}$	Vector containing daily simulated water levels at WL IN_2 for the year y
$\sigma0_y$	Vector containing the daily weights of the suspicious measures located in $Z0_{obs,y}$
$\sigma2_y$	Vector containing the daily weights of the suspicious measures located in $Z1_{obs,y}$, $Z2_{obs,y}$ and $Z4_{obs,y}$
$\sigma3_y$	Vector containing the daily weights of the suspicious measures located in $Z1_{obs,y}$, $Z3_{obs,y}$ and $Z4_{obs,y}$

References

1. Sun, H.; Wang, S.; Hao, X. An Improved Analytic Hierarchy Process Method for the evaluation of agricultural water management in irrigation districts of north China. *Agric. Water Manag.* **2017**, *179*, 324–337. [CrossRef]
2. Chen, S.; Ravallion, M. *Absolute Poverty Measures for the Developing World, 1981–2004*; PNAS: Washington, DC, USA, 2007.
3. European Commission. *Roadmap to a Resource Efficient Europe*; European Environment Agency: Brussels, Belgium, 2011; pp. 1–24.
4. Gordon, L.J.; Finlayson, C.M.; Falkenmark, M. Managing water in agriculture for food production and other ecosystem services. *Agric. Water Manag.* **2010**, *97*, 512–519. [CrossRef]
5. De Fraiture, C.; Molden, D.; Wichelns, D. Investing in water for food, ecosystems, and livelihoods: An overview of the comprehensive assessment of water management in agriculture. *Agric. Water Manag.* **2010**, *97*, 495–501. [CrossRef]
6. European Environmental Agency (EEA). *Water Resources Across Europe-Confronting Water Scarcity and Drought*; European Environment Agency: Copenhagen, Denmark, 2009; pp. 1–55.
7. Molden, D. *Water for Food, Water for Life: A Comprehensive Assessment of Water Management in Agriculture*; Earthscan, IWMI: London, UK, 2007; pp. 1–39.
8. Namara, R.E.; Hanjra, M.A.; Castillo, G.E.; Ravnborg, H.M.; Smith, L.; Koppen, B.V. Agricultural water management and poverty linkages. *Agric. Water Manag.* **2010**, *97*, 520–527. [CrossRef]
9. Barker, R.; Molle, F. Evolution of irrigation in South and Southeast Asia, 2004. Available online: https://www.eea.europa.eu/publications/water-resources-across-europe (accessed on 27 July 2018).
10. European Commission. Directive 2000/60/EC of the European Parliament and of the Council Establishing a Framework for the Community Action in the Field of Water Policy. Available online: https://www.eea.europa.eu/policy-documents/directive-2000-60-ec-of (accessed on 27 July 2018).
11. European Commission DG ENV. *Water Saving Potential in Agriculture in Europe: Findings from the Existing Studies and Applications*; BIO Intelligence Service: Paris, France, 2012; pp. 1–232.
12. Masseroni, D.; Ricart, S.; de Cartagena, F.; Monserrat, J.; Gonçalves, J.; de Lima, I.; Facchi, A.; Sali, G.; Gandolfi, C. Prospects for Improving Gravity-Fed Surface Irrigation Systems in Mediterranean European Contexts. *Water* **2017**, *9*, 20. [CrossRef]

13. Levidow, L.; Zaccaria, D.; Maia, R.; Vivas, E.; Todorovic, M.; Scardigno, A. Improving water-efficient irrigation: Prospects and difficulties of innovative practices. *Agric. Water Manag.* **2014**, *146*, 84–94. [CrossRef]

14. Ministero delle Politiche Agricole Alimentari e Forestali (MiPAAF). *Approvazione delle linee guida per la regolamentazione da parte delle Regioni delle Modalità di quantificazione dei volumi idrici ad uso irriguo*; MiPAAF: Rome, Italy, 2015.

15. Litrico, X.; Fromion, V.; Baume, J.-P.; Arranja, C.; Rijo, M. Experimental validation of a methodology to control irrigation canals based on Saint-Venant Equations. *Control Eng. Pract.* **2005**, *13*, 1425–1437. [CrossRef]

16. Lozano, D.; Arranja, C.; Rijo, M.; Mateos, L. Simulation of automatic control of an irrigation canal. *Agric. Water Manag.* **2010**, *97*, 91–100. [CrossRef]

17. Cantoni, M.; Weyer, E.; Li, Y.; Ooi, S.K.; Mareels, I.; Ryan, M. Control of Large-Scale Irrigation Networks. *Proc. IEEE* **2007**, *95*, 75–91. [CrossRef]

18. Ooi, S.K.; Weyer, E. Control design for an irrigation channel from physical data. *Control Eng. Pract.* **2008**, *16*, 1132–1150. [CrossRef]

19. Jean-Baptiste, N.; Malaterre, P.-O.; Dorée, C.; Sau, J. Data assimilation for real-time estimation of hydraulic states and unmeasured perturbations in a 1D hydrodynamic model. *Math. Comput. Simul.* **2011**, *81*, 2201–2214. [CrossRef]

20. Jeroen, V.; Linden, V. Volumetric water control in a large-scale open canal irrigation system with many smallholders: The case of chancay-lambayeque in Peru. *Agric. Water Manag.* **2011**, *98*, 705–714.

21. Islam, A.; Raghuwanshi, N.S.; Singh, R. Development and application of hydraulic simulation model for irrigation canal network. *J. Irrig. Drain. Eng.* **2008**, *134*, 49–59. [CrossRef]

22. Renault, D. Aggregated hydraulic sensitivity indicators for irrigation system behavior. *Agric. Water Manag.* **2000**, *43*, 151–171. [CrossRef]

23. Cornish, G.; Bosworth, B.; Perry, C.; Burke, J. Water Charging in Irrigated Agriculture: An Analysis of International Experience. Available online: http://www.fao.org/docrep/008/y5690e/y5690e00.htm (accessed on 6 June 2018).

24. Laycock, A. *Irrigation Systems: Design, Planning and Construction*; CAB International: Wallingford, UK, 2007; pp. 1–285.

25. Molle, F. Water scarcity, prices and quotas: A review of evidence on irrigation volumetric pricing. *Irrig. Drain. Syst.* **2009**, *23*, 43–58. [CrossRef]

26. Food and Agriculture Organization of the United Nations (FAO). *The State of the World's Land and Water Resources for Food and Agriculture (SOLAW)—Managing Systems at Risk*; Food and Agriculture Organization of the United Nations: Rome, Italy, 2011; pp. 1–281.

27. Rault, P.K.; Jeffrey, P. On the appropriateness of public participation in integrated water resources management: Some grounded insights from the Levant. *Integr. Assess.* **2008**, *8*, 69–106.

28. Huang, Y.; Fipps, G. Developing a modeling tool for flow profiling in irrigation distribution networks. *Int. J. Agric. Biol. Eng.* **2009**, *2*, 17–26.

29. Tariq, J.A.; Latif, M. Improving operational performances of farmers managed distributary canal using SIC hydraulic model. *Water Resour. Manag.* **2010**, *24*, 3085–3099. [CrossRef]

30. Sau, J.; Malaterre, P.O.; Baume, J.P. Sequential Monte Carlo hydraulic state estimation of an irrigation canal. *Comptes Rendus Mécanique* **2010**, *338*, 212–219. [CrossRef]

31. Kumar, P.; Mishra, A.; Raghuwanshi, N.S.; Singh, R. Application of unsteady flow hydraulic-model to a large and complex irrigation system. *Agric. Water Manag.* **2002**, *54*, 49–66. [CrossRef]

32. Giupponi, C. Decision Support Systems for implementing the European Water Framework Directive: The MULINO approach. *Environ. Model. Softw.* **2007**, *22*, 248–258. [CrossRef]

33. Mateos, L.; Lopez-Cortijo, I.; Sagardoy, J. SIMIS the FAO decision support system for irrigation scheme management. *Agric. Water Manag.* **2002**, *56*, 193–206. [CrossRef]

34. Leenhardt, D.; Trouvat, J.L.; Gonzalès, G.; Pérarnaud, V.; Prats, S.; Bergez, J.E. Estimating irrigation demand for water management on a regional scale. *Agric. Water Manag.* **2004**, *68*, 207–232. [CrossRef]

35. Mailhol, J.-C. *Evaluation à l'échelle Régionale des Besoins en Eau et du Rendement des Cultures Selon la Disponibilité en eau. Application au bassin Adour-Garonne*; Agence de l'Eau Adour-Garonne: Toulouse, France, 1992; pp. 1–24.

36. Sousa, V.; Santos Pereira, L. Regional analysis of irrigation water requirements using kriging. Application to potato crop (*Solanum tuberosum* L.) at Tras-os-Montes. *Agric. Water Manag.* **1999**, *40*, 221–233. [CrossRef]

37. Heinemann, A.B.; Hoogenboom, G.; Faria de, R.T. Determination of spatial water requirements at county and regional levels using crop models and GIS: An example for the state of Parana, Brazil. *Agric. Water Manag.* **2002**, *52*, 177–196. [CrossRef]

38. Kinzli, K.-D.; Gensler, D.; Oad, R.; Shafike, N. Implementation of a decision support system for improving irrigation water delivery: Case study. *Irrig. Drain. Syst.* **2015**, *141*, 05015004. [CrossRef]

39. Miao, Q.; Shi, H.; Gonçalves, J.; Pereira, L. Basin irrigation design with multi-criteria analysis focusing on water saving and economic returns: Application to wheat in Hetao, Yellow River Basin. *Water* **2018**, *10*, 67. [CrossRef]

40. Yang, G.; Liu, L.; Guo, P.; Li, M. A flexible decision support system for irrigation scheduling in an irrigation district in China. *Agric. Water Manag.* **2017**, *179*, 378–389. [CrossRef]

41. Tanure, S.; Nabinger, C.; Becker, J.L. Bioeconomic model of decision support system for farm management: Proposal of a mathematical model: Bioeconomic model of decision support system for farm management. *Syst. Res. Behav. Sci.* **2015**, *32*, 658–671. [CrossRef]

42. Consortium of the Canale Emiliano Romagnolo (CER). Available online: http://www.consorziocer/ (accessed on 17 May 2018).

43. Istituto Nazionale di Statistica (ISTAT). Censimento Agricoltura 2010. Available online: http://www4.istat.it/it/censimento-agricoltura/agricoltura-2010 (accessed on 22 May 2018).

44. Munaretto, S.; Battilani, A. Irrigation water governance in practice: The case of the Canale Emiliano Romagnolo district, Italy. *Water Policy* **2014**, *16*, 578. [CrossRef]

45. Service IRRIFRAME. Available online: https://ssl.altavia.eu/Irriframe/ (accessed on 29 October 2017).

46. Delibera di Giunta Regionale (DGR). *Bollettino Ufficiale della Regione Emilia Romagna, Parte Seconda, n.9—Deliberazione della Giunta Regionale 21 Dicembre 2016, n. 2254*; Giunta Regionale: Bologne, Italy, 2016; pp. 1–10. (In Italian)

47. Mannini, P.; Genovesi, R.; Letterio, T. IRRINET: Large scale DSS application for on-farm irrigation scheduling. *Procedia Environ. Sci.* **2013**, *19*, 823–829. [CrossRef]

48. Singley, B.C.; Hotchkiss, R.H. Differences between Open-Channel and Culvert Hydraulics: Implications for Design. 2010. Available online: https://doi.org/10.1061/41114 (accessed on 27 July 2018).

49. Software SIC2. Available online: http://sic.g-eau.net/ (accessed on 30 October 2017).

50. Haque, S. Impact of irrigation on cropping intensity and potentiality of groundwater in murshidabad district of West Bengal, India. *Int. J. Ecosyst.* **2015**, *5*, 55–64.

51. Thenkabail, P.; Dheeravath, V.; Biradar, C.; Gangalakunta, O.R.; Noojipady, P.; Gurappa, C.; Velpuri, M.; Gumma, M.; Li, Y. Irrigated area maps and statistics of India using remote sensing and national statistics. *Remote Sens.* **2009**, *1*, 50–67. [CrossRef]

52. Tanriverdi, C.; Degirmenci, H.; Sesveren, S. Assessment of irrigation schemes in Turkey: Cropping intensity, irrigation intensity and water use. In Proceedings of the Tropentag 2015, Berlin, Germany, 16–18 September 2015.

53. Battilani, A. L'irrigazione del medicaio. *Agricoltura* **1994**, *3*, 31–33.

54. Battilani, A. Regulated deficit of irrigation (RDI) effects on growth and yield of plum tree. *Acta Hortic.* **2004**, *664*, 55–62. [CrossRef]

55. Battilani, A.; Anconelli, S.; Guidoboni, G. Water table level effect on the water balance and yield of two pear rootstock. *Acta Hortic.* **2004**, *664*, 47–54. [CrossRef]

56. Battilani, A.; Ventura, F. Influence of water table, irrigation and rootstock on transpiration rate and fruit growth of peach trees. *Acta Hortic.* **1996**, *449*, 521–528. [CrossRef]

57. Food and Agriculture Organization of the United Nations (FAO). Irrigation Water Management: Irrigation Scheduling, Training Manual n.4. 1989. Available online: http://www.fao.org/docrep/t7202e/t7202e08.htm (accessed on 21 June 2017).

58. Delibera di Giunta Regionale (DGR). *Bollettino Ufficiale della Regione Emilia Romagna, Parte Seconda, n.327—Deliberazione della Giunta Regionale 5 Settembre 2016, n. 1415*; Giunta Regionale: Bologne, Italy, 2016; pp. 1–11. (In Italian)

59. Artina, S.; Montanari, A. *Consulenza per lo Studio delle Perdite Idriche nelle Reti di Distribuzione dei Consorzi di Bonifica*; Università degli Studi di Bologna: Bologne, Italy, 2007; pp. 1–46. (In Italian)

60. Taglioli, G.; Cinti, P. Water Losses of Land Channels [Emilia-Romagna]. *Rivista di Ingegneria Agraria*. 2002. Available online: http://agris.fao.org/agris-search/search.do?recordID=IT2004060023 (accessed on 27 July 2018).

61. Consorzio della Bonifica Renana. Available online: https://www.bonificarenana.it/ (accessed on 11 July 2018).
62. Gejadze, I.; Malaterre, P.O. Discharge estimation under uncertainty using variational methods with application to the full Saint-Venant hydraulic network model: Discharge estimation under uncertainty using variational methods. *Int. J. Numer. Methods Fluids* **2017**, *83*, 405–430. [CrossRef]
63. Oubanas, H.; Gejadze, I.; Malaterre, P.O. River discharge estimation under uncertainty from synthetic SWOT-type observations using variational data assimilation. Contribution of the UMR G−eau investigation team, IRSTEA Montpellier, France to the SWOT mission. *La Houille Blanche* **2018**, *2*, 84–89. [CrossRef]
64. Baume, J.P.; Malaterre, P.O.; Benoit, G.B. *SIC: A 1D Hydrodynamic Model for River and Irrigation Canal Modeling and Regulation*; CEMAGREF, Agricultural and Environmental Engineering Research: Montpellier, France, 2005; pp. 1–81.
65. Sau, J.; Malaterre, P.-O.; Baume, J.P. Sequential Monte Carlo hydraulic state estimation of an irrigation canal. *Comptes Rendus Mécanique* **2010**, *338*, 212–219. [CrossRef]
66. Cunge, J.; Holly, F.M.; Verwey, A., Jr. *Practical Aspects of Computational Rive Hydraulics*; Pitman Advanced Pub. Program: Boston, MA, USA, 1980; pp. 1–420.
67. Chaudhry, H.M. *Open Channel Flow*, 2nd ed.; Springer: New York, NY, USA, 2007; pp. 1–517.
68. Baume, J.-P.; Belaud, G.; Vion, P.Y. *Hydraulique Pour le Génie Rural Notes de Cours*; Ecole Nationale Supérieure d'Agronomie, CEMAGREF: Montpellier, France, 2006; pp. 1–179.
69. Nielsen, K.D.; Weber, L.J. Submergence effects on discharge coefficients for rectangular. In Proceedings of the Joint Conference on Water Resource Engineering and Water Resources Planning and Management 2000, Minneapolis, MN, USA, 30 July–2 August 2000.
70. Nelder, J.A.; Mead, R. A simplex method for function minimization. *Comput. J.* **1965**, *7*, 308–313. [CrossRef]
71. United States Bureau of Reclamation (USBR). *Water Measurement Manual*; Water Resources: Englewood, CO, USA, 1997.
72. Wu, S.; Rajaratnam, N. Solutions to rectangular sluice gate flow problems. *J. Irrig. Drain. Eng.* **2015**, *141*, 06015003. [CrossRef]
73. Sauida, M.F. Calibration of submerged multi-sluice gates. *Alexandria Eng. J.* **2014**, *53*, 663–668. [CrossRef]
74. Chow, V.T. *Open-Channel Hydraulics*; McGraw-Hill: New York, NY, USA, 1959; pp. 1–680.
75. De Doncker, L.; Troch, P.; Verhoeven, R.; Bal, K.; Meire, P.; Quintelier, J. Determination of the manning roughness coefficient influenced by vegetation in the river Aa and Biebrza river. *Environ Fluid Mech.* **2009**, *9*, 549–567. [CrossRef]
76. Dyhouse, G.; Hatchett, J.; Benn, J. *Floodplain Modeling Using HEC-RAS*; Haestad Press: Aterbury, CT, USA, 2003; pp. 1–1261.
77. Tedeschi, L.O. Assessment of the adequacy of mathematical models. *Agric. Syst.* **2006**, *89*, 225–247. [CrossRef]
78. St-Pierre, N.R. Comparison of model predictions with measurements: A novel model-assessment method. *J. Dairy Sci.* **2016**, *99*, 4907–4927. [CrossRef] [PubMed]
79. Harrison, S.R. Validation of agricultural expert systems. *Agric. Syst.* **1991**, *35*, 265–285. [CrossRef]
80. Mayer, D.G.; Butler, D.G. Statistical validation. *Ecol. Model.* **1993**, *68*, 21–32. [CrossRef]
81. Mayer, D.G.; Stuart, M.A.; Swain, A.J. Regression of real-world data on model output: An appropriate overall test of validity. *Agric. Syst.* **1994**, *45*, 93–104. [CrossRef]
82. Dent, J.B.; Blackie, M.J. *Systems Simulation in Agriculture*; Applied Science: London, UK, 1979.
83. Mesplé, F.; Troussellier, M.; Casellas, C.; Legendre, P. Evaluation of simple statistical criteria to qualify a simulation. *Ecol. Model.* **1996**, *88*, 9–18. [CrossRef]